Semiconductor track detectors

V. G. Sandukovskiĭ
Joint Institute for Nuclear Research, Dubna

V. I. Savel'ev
Engineering-Physics Institute, Moscow

Fiz. Elem. Chastits At. Yadra **22**, 1347–1399 (November–December 1991)

The present status of investigations in the development of various types of semiconductor position-sensitive detectors is reviewed. Particular attention is devoted to miniaturized types of discrete devices: microstrip detectors, charge-coupled devices, and drift chambers. The advantages and shortcomings of the various types of detector are analyzed, and methods of optimizing their main parameters—spatial resolution, double-particle resolution, readout time, and number of signal outputs—are considered. The various readout methods, the requirements on the primary electronics, the conditions of optimal analysis of signals from the detectors, and the latest achievements in the application of multichannel monolithic integrated readout electronics are described. The effects of radiation and magnetic fields on the detector parameters are considered. Examples of the use of semiconductor track systems in some modern experiments are given.

INTRODUCTION

Semiconductor detectors of nuclear radiations, which are capable of giving information about the tracks of particles (in what follows, we shall refer to them by the abbreviation STD: semiconductor track detectors), have become firmly established in modern experimental technology. Several advantages of these devices, above all the high spatial (and in individual cases, also energy) resolution, miniaturization, the ability to operate in magnetic fields and in vacuum, and other qualities, explain the growing interest of investigators in them.

Progress in the technology of obtaining high-quality single crystals, and also the penetration of the methods of microelectronics into the technology of the manufacture of semiconductor detectors have stimulated many developments in the construction and use of STDs in experimental nuclear physics.

The currently existing types of STD differ not only in the geometry, technology of fabrication, and readout method, but also in the principles of operation. Therefore, when an experiment is being planned, the optimal choice of the detecting systems arises. It is here necessary to take into account (besides the spectrometric capabilities of the different types of STD) the problem of the actual accessibility and cost of the detectors themselves as well as the corresponding readout electronics. It is obvious that an understanding of the principles of operation of the different detectors and knowledge of their comparative characteristics and detecting capabilities are necessary in the planning of investigations and the performance of measurements.

It will be easier to form a picture of the various types of STD if we distinguish the three main classes of devices: continuous, discrete, and single-crystal devices. In the continuous STDs, the main element is a resistive electrode. The division in it of the charge formed by a particle in the volume of the detector makes it possible to extract information about the position at which the particle passed. In discrete STDs, the individual detecting elements are situated in a common single crystal. The position information is determined by the positions of the elements that respond. Single-crystal STDs are devices consisting of matrices (hodoscopes) or multilayer "sandwiches" (telescopes, calorimeters) of independent semiconductor detectors.

Until the end of the seventies, the developments of the STDs were largely associated with their use in experiments in low-energy physics, for which it was not necessary (in contrast to the spectrometers used in high-energy physics experiments) to have large detection areas and volumes. The spatial resolution of the STDs (0.1–5 mm), coupled with the comparatively modest electronics, satisfied the requirements of the experimentalists.

The discovery of charmed, and then beauty particles, which have a lifetime of about 10^{-13} sec, created a need for small detectors that could be placed very close to the interaction region and possessed a spatial resolution at the micron level. In addition, it was desirable to have the possibility of detecting many particles and organizing an electronic trigger. Searches led to the development in experimental nuclear physics of miniaturized discrete STDs—microstrip detectors, charge-coupled devices, and drift chambers.

The rapid progress during the last decade observed in the development of miniaturized STDs and the corresponding readout electronics was due, in particular, to the use of the methods and technological devices developed in the microelectronics industry in the fabrication of semiconductor detectors.

A considerable number of scientific publications have been devoted to the methods of producing the various types of STD, the necessary electronics, and applications in experiments. Some reviews have discussed individual classes of STDs, for example, continuous,[1,2,3] miniaturized discrete,[4–11] and single-crystal devices.[12] There have been interesting publications about STDs that realize nontraditional principles of particle-track detection, for example,

 0090-4759/91/060655-26$04.00 © 1992 American Institute of Physics

devices that produce an image of the tracks,[13] detectors with cryogenic charge storage,[14] and microelectrode matrices with individual addressing and data analysis of each detecting element integrated in one crystal.[15,16]

In this paper, we consider the various types of STD and compare their properties. The main attention will be devoted to miniaturized discrete devices. Sections 2–4 are devoted to a description of the principles of operation and the methods of fabrication of the well-known types of STD. Section 5 discusses aspects of the supporting electronics of the detectors. Section 6 considers the effect of external factors (radiation, magnetic fields, etc.) on the operation of the devices. Section 7 gives examples of the use of miniaturized STDs in modern experiments.

1. GENERAL REMARKS

The operation of any semiconductor detector is based on detection of the charge produced by an ionizing particle in a region of the detector depleted of charge carriers (in a semiconductor, these are electrons and holes). The depletion is achieved by creating a diode structure which operates in the "barrier" regime. The most important parameters of any type of STD are: the spatial resolution; the energy resolution (only for certain types of STD); the double-particle resolution (the minimal separation between two simultaneously detected particles that can be distinguished by the STD); the time of information readout from the detector; the number of signal outputs.

The desire of users and, therefore, the developers of the devices to minimize these parameters is obvious. In considering the different types of detectors in what follows, this is the point of view that we shall adopt. We shall not consider in detail the choice of the original single crystals and the testing of their properties. This is the subject of a separate discussion, which can be found, for example, in Ref. 17. We merely mention that for most STDs one requires single crystals of high-resistivity silicon (for n-type Si, resistivity $\rho > 2$ kΩ·cm) or high-purity germanium (HP Ge), which have long carrier lifetimes (of order 1 msec at room temperature) and high uniformity of the parameters in the employed volume of the crystal. An important part in semiconductor detectors is played by the contacts, which must be minimally thin "dead" layers for the detected radiations and at the same time should not permit injection of carriers into the (carrier-depleted) working region of the device at electric field strengths of 10^3–10^4 V/cm.

2. CONTINUOUS DETECTORS

Historically, the development of continuous STDs was stimulated by the desire to have an electronic solution to the problem of detecting particles in magnetic spectrographs[18] in order to obtain data in the on-line regime, in contrast to the method using photographic plates. In addition, the possibility appeared of simultaneously obtaining information on the energy of the detected particles, so that their species could be identified.

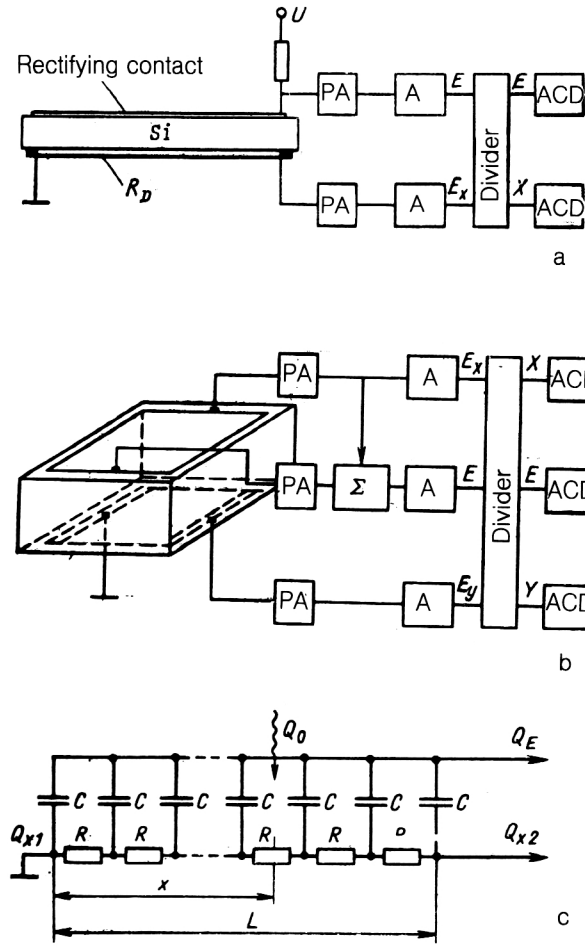

FIG. 1. Structure of a continuous semiconductor track detector and circuit of the pulse-height method of signal readout: a) single-coordinate detector; b) two-coordinate detector; c) equivalent circuit of detector in the form of a continuously distributed RC line.

The principle of operation of a continuous STD is based on resistive division of the charge produced by a particle (Fig. 1). Single- and two-coordinate constructions of the device are possible. If the resistivity of the resistive electrode is uniform over the surface, and amplifiers with low input impedance are used, then the charge taken from one of the ends of the electrode will be exactly proportional to the distance between the point at which the particle passed and the other (grounded) end of the electrode (Fig. 1c), i.e., $Q_x = QX/L$. This is the case in the so-called pulse-height method of signal readout. The other, time method[19] (which uses the difference between the times of arrival of the signals at the edges of the electrode) was not widely used in continuous STDs because of the large noise contribution and the stringent requirements on filtering of the signals to obtain a linear response.[2]

In the development of continuous STDs, it is obviously desirable to produce resistive layers that are maximally uniform over their area. The greatest uniformity is achieved by using the methods of diffusion and ion implantation. The layer resistance usually achieved is in the range 10–100 kΩ. The detector sizes are limited by the dimen-

sions of the original material with the required parameters. At the present time, it is possible to fabricate continuous silicon STDs with dimensions up to 100 mm and 50×50 mm, respectively, for the single- and two-coordinate types. We mention that the commercially available detectors, fabricated, for example, by the firms ORTEC and Schlumberger, are, as a rule, single-coordinate devices measuring from 10×8 to 50×8 mm with thickness 100–1000 μm of the working region. The cost of such detectors is \$2000–10 000.

Basic characteristics

The normal operation of continuous STDs is based on fulfillment of requirements on the signal shaping, the optimization of which is governed by the relationship between the linearity and the resolution of the device.

In the considered type of device, the *detector linearity* depends on the ratio τ/R_DC_D, where τ is the time constant of the shaping circuits of the amplifier, R_D is the resistance of the resistive electrode, and C_D is the capacitance of the detector. The difference between the signal rise times, given the restrictions on the shaping constants τ, leads to a ballistic deficit—a difference at the amplifier output between a step signal and a signal having a rise front of the same pulse height. The consequence of this is nonlinearity of the response of both the position and energy outputs. The linearity also depends on the type of shaping circuits, i.e., on the transfer function of the amplifier. Investigations made for amplifiers with different signal shaping[21] (with single differentiation and single integration, single differentiation and double integration, with filters giving a trapeziform pulse shape, and with active filters) show that without a large error one can assume that a system is linear (nonlinearity not greater than 1%) if the condition

$$R_DC_D \leqslant 2\tau$$

is satisfied. Normalization of the position signal by means of a divider (Figs. 1a and 1b) not only eliminates a dependence of the position information on the energy but also reduces the nonlinearity, for example, from 4 to 1%.

Spatial resolution. Analysis of the operation of a continuous STD on the basis of a model of the detector in the form of a distributed RC line[20] (see Fig. 1c) shows that the spatial resolution of such devices can be estimated by means of the expression

$$\sigma = \sigma_n L/E,$$

where σ_n is the total noise, including the contributions of the electronics, the detector leakage currents, and the thermal noise of the resistive electrode; L is the length of the resistive electrode; and E is the energy of the particle absorbed by the detector. The noise of the resistive layer of the detector is proportional to $(\tau/R_D)^{1/2}$, and the noise of the leakage currents is proportional to $(I_D\tau)^{1/2}$. Therefore, the desire to use a large τ and small R_D in order to obtain linearity comes into conflict with the desire to have a low-noise contribution, which requires short signal-shaping times and large R_D. The optimal choice depends on the requirements of the particular experiment. In the majority of cases, involving the use of standard continuous STDs and preamplifiers, the FWHM of the noise distribution for the position output lies in the range 30–60 keV (for silicon). As an example, Fig. 2 shows the behavior of the noise of the position and energy outputs as a function of R_D ($C_D = 100$ pF, $\tau = 1$ μsec, i.e., the conditions of linearity are satisfied up to $R_D = 20$ kΩ). For α particles ($E = 5$ MeV), this leads to a position resolution with FWHM $\simeq 1\%$ of the length (L) of the resistive layer.

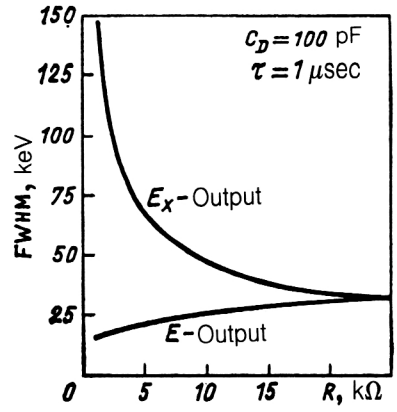

FIG. 2. Dependence of the noise of position (E_x) and energy (E) outputs on the resistance of the resistive electrode.

The *energy resolution* is basically determined by the noise of the detector leakage currents and the capacitance at the preamplifier input (in the first place, this is the detector capacitance C_D). The planar technology developed by Kemmer[22] for silicon detectors (see Sec. 2) makes it possible to lower significantly the noise contribution of the leakage currents. Another way of reducing the currents is to cool the detector. In conjunction with special preamplifiers designed for large input capacitances, for example, the ones shown in Ref. 23, one can expect to obtain for large detectors (area of order 20 cm^2) a resolution (FWHM) of order 40–50 keV for α particles ($E_\alpha = 5$ MeV).

The *readout time* of continuous STDs is determined by the maximal signal rise time, which depends on R_D and C_D ($t = 0.5R_DC_D$). For detectors having capacitance $C_D \simeq 1000$ pF, t may reach 5 μsec.

Applications. Advantages and shortcomings

Continuous STDs are used above all to detect strongly ionizing, short-range particles, for which their spatial resolution is best realized. If a short readout time is not required, the simplicity of the electronics compared with discrete STDs may be a decisive factor in the choice of the detector. We shall give only a few examples of the use of continuous STDs in experiments: in a magnetic spectrograph,[24] in which a set of detectors covered part of the focal plane; in a study of fission in reactions induced by neutrons and heavy ions;[25] in the investigation of the correlation spectra of α particles and fission fragments in the $^{12}C + ^{232}Th$ reaction.[26] Continuous detectors are also used

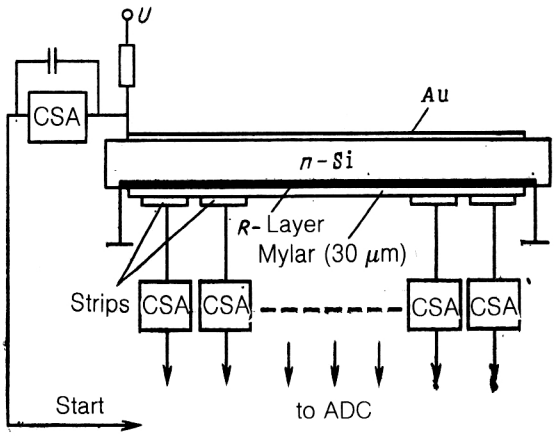

FIG. 3. Continuous STD with external system of signal strip electrodes (pitch of electrodes 0.5 μm, duration of strobing pulse plus delay time 50–150 nsec).[31]

to detect γ rays (STDs made from HP Ge)[27] and in electron spectrometry [Si(Li) detector].[28] Radially sensitive continuous STDs,[29] in particular, with a linear response function,[30] can also have a certain interest.

Hitherto, we have discussed charge readout directly from a resistive electrode. Another possibility is when the information readout is done by means of an external system of signal strip electrodes on which a charge distribution formed by an RC line is induced (Fig. 3).[31] The spatial resolution of such a device (experimentally, $\sigma=25$ μm for strip pitch 0.5 mm has been obtained) is not inferior to that of microstrip detectors (see Sec. 3) with a significantly smaller number of outputs of the readout electronics. The readout time of such a system is several times higher than that of standard continuous STDs.

The main advantage of the standard continuous STDs—the simplicity of the electronics for the readout—is not always the main argument in the choice of a track detector. When measurements are made that require a high counting rate, and also time information (coincidence experiments), it must be borne in mind that in continuous STDs only one event can be analyzed at a given time. Moreover, the readout time in detectors with area 10–20 cm^2 of the working surface is several microseconds. A further shortcoming is the dependence of the spatial resolution on the dimensions of the resistive layer, i.e., the dimensions of the detector, and on the energy loss of the particle in the detector. Estimates show that for detectors measuring 50×50 mm and with thickness $d=1$ mm of the working region one can expect a spatial resolution (FWHM) for α particles ($E_\alpha = 5$ MeV) not better than 0.5 mm, and for relativistic, i.e., minimally ionizing particles, not better than 10 mm. Therefore, in experiments in which there is a need for high load characteristics, fast readout, and detection of low-energy radiations, discrete STDs are preferable.

3. DISCRETE DETECTORS

In devices of this type, the individual detecting elements (diode structures) are arranged on a common base material. The elements can be arranged in the form of strips or cells. Detectors with strip structure of the elements are often called strip detectors. The first strip detector was already demonstrated[32] in 1966. Detectors having strips from 0.5 to 3 mm and fabricated by the standard technology for obtaining silicon and germanium detectors were mainly used in low-energy nuclear physics. Detectors of both the single-coordinate[33] and two-coordinate[34] (orthogonal arrangement of strips on the front and back sides of the crystal) type are possible.

The requirements of high-energy physics, in particular the need to reconstruct with micron accuracy the topology of an event in investigations of charmed and beauty particles, stimulated the development of miniaturized discrete STDs. Three concepts of miniaturized discrete STDs achieved the greatest progress: microstrip detectors (MSD), detectors based on charge-coupled devices (CCD detectors), and semiconductor drift chambers (SDC).

Despite the differences in the principles of operation of these types of detector, a feature that they have in common is the presence of an appreciable number of detecting elements. Depending on the type of detector, this number varies from 10^2 to 10^6. This "subdivision" of the STD structure arises from the desire to exploit to the maximum possible extent the potential advantages in obtaining spatial resolution. Obviously, there is then a problem of the optimum solution for the readout problem. Therefore, besides the spatial resolution and multiparticle resolution, an important parameter of miniaturized STDs is the number of readout outputs and, as a consequence, the readout time of the device. The desire to achieve the best readout time requires parallel readout of signals, and this leads to a large number of outputs of the readout electronics. On the other hand, the desire to realize the readout with as few outputs as possible leads to a sequential process of signal processing and, accordingly, to an increase of the readout time. Another important parameter for all semiconductor detectors is the signal-to-noise ratio (Q_0/σ_n). This parameter determines the direction in which the readout electronics is developed.[36]

The search for optimum relationships between the above-mentioned parameters is the basis of the development of the various concepts for developing miniaturized discrete STDs.

Microstrip detectors

A microstrip detector is a plane-parallel semiconductor detector in which one or two electrodes are made in the form of strips having width and position periodicity in the range from 10 to 1000 μm. The main geometrical parameters of microstrip detectors on which the spatial resolution depends are the strip width W, the pitch (distance between the centers of the strips) $S=W+b$, and the depth d of the depleted region (as a rule, the thickness of

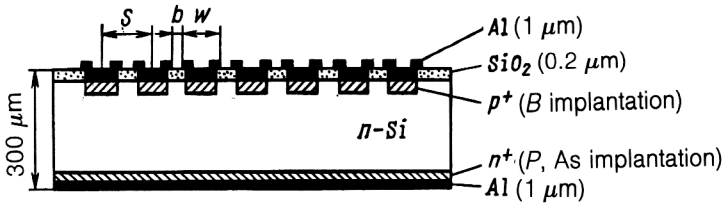

FIG. 4. Structure of a standard microstrip detector (S is the strip pitch, b is the interstrip separation, and W is the strip width).

the MSD). Of no small importance is the active area A of the detector, which determines its geometrical efficiency.

The first examples of MSDs of two types were demonstrated[36] in 1980. These detectors, fabricated using the standard surface-barrier method, had thickness 400 μm, a working surface measuring 20×30 mm of 100 strips with width 140 μm, length 30 mm, and pitch 2000 μm. The detectors of one type had gold strips on the side of the rectifying contact and a continuous aluminum ohmic contact on the opposite side. The other type had aluminum strips and a continuous rectifying electrode. At the voltage of complete depletion (110 V), the detectors exhibited total leakage currents as follows: from the gold strips about 2 μA, and from the aluminum strips about 1 μA. Tests made with these detectors in a pion beam (175 GeV/c) at CERN showed that their efficiency was 99.6%. Unfortunately, the surface-barrier technology did not make it possible to obtain devices that were sufficiently reliable for prolonged operation.

The introduction of the planar technology[22] in the fabrication of semiconductor detectors opened the way to the development of more reliable and more accurate MSDs. Figure 4 gives an idea of the structure of a typical MSD fabricated by the planar technology. The basis of the detector is a wafer of (n-type) silicon with resistivity $\rho>3$ k$\Omega\cdot$cm, this making it possible to achieve complete depletion of detectors of width more than 200 μm at working voltages $U\simeq100$ V [$d=0.53(\rho U)^{1/2}$, where d is measured in μm, σ in $\Omega\cdot$cm, and U in V].

The sequence of processes in the treating of the silicon wafer (Fig. 5) includes oxide passivation of the surface, photolithography, ion implantation, and metallization of the strips.

Oxide passivation is an effective method of lowering the reverse currents (and, therefore, the detector noise), making it possible to obtain currents less than 10 nA/cm^2 for silicon of thickness 100 μm. The reason for this is that thermal oxidation of the silicon (1000–1100 °C) in an atmosphere of oxygen with a small admixture of HCl not only significantly reduces the surface leakage currents, but also leads, as Kemmer showed,[22] to an increase in the volume lifetime τ_q of the charge carriers, i.e., to smaller volume generation–recombination currents (I_{gen} is inversely proportional to τ_q).

Ion implantation makes it possible, for correct choice of the parameters (implanation energy and dose), to make abrupt p–n junctions, i.e., thin entrance windows of the detectors. For n-Si rectifying contacts, boron ions (energy 10–15 keV, dose 5×10^{14} cm^{-2}) are usually used. An ohmic contact (n^+) is obtained by implanting phosphorous or arsenic ions (energy 30 keV, dose 5×10^{15} cm^{-2}). The thickness of the implanted electrodes is in the range 0.05–0.1 μm. To eliminate channeling effects, the implantation is made at small angles to the ⟨111⟩ axis, in the direction of which the silicon wafer is, as a rule, oriented.

Metallization of the p^+ and n^+ electrodes of a microstrip detector makes it possible to avoid problems of surface resistance and to improve the external electric contacts. Photolithography makes it possible to create an accurate configuration of the strips and carry out selectively technological operations on the required sections of the silicon sample.

An important parameter for experimentalists is the

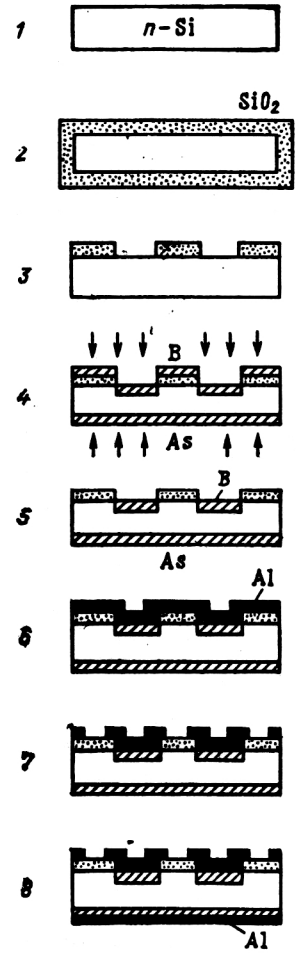

FIG. 5. Sequence of processes of fabrication of microstrip detectors in accordance with the planar technology.[22]

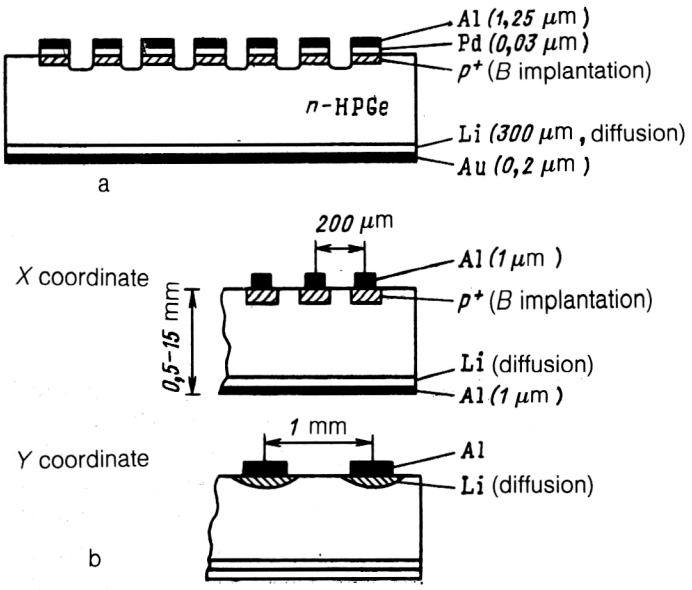

FIG. 6. Structures of HP Ge microstrip detectors: a) detectors developed for the active target of the NA1 experiment at CERN (Ref. 38); b) the MSDs fabricated by the firm Intertechnique (France).[39]

size of the sensitive region of the detector. The area of the working surface of MSDs is limited by the diameter of the single crystals of the silicon produced by industry that is suitable for making detectors. At the present time, the maximum silicon diameter does not exceed 10 cm, and this makes it possible to obtain MSDs with dimensions up to 70×70 mm. Such silicon with the necessary resistivity and carrier lifetime is still difficult to obtain, and in the technology material with diameter up to 76 mm is mainly used. The minimum thickness of an MSD (without allowance for the mechanical strength of the silicon wafer) is determined by the need to obtain at the preamplifier input a charge sufficient for reliable readout. The typical thickness of MSDs fabricated by the planar technology is $d=300$ μm.

During the last decade, a considerable number of publications have been devoted to the development and fabrication of MSDs. We shall consider some of the papers that discuss features different from the technology for fabricating standard MSDs. The MSD discussed in Ref. 37 has capacitative coupling, a strip preamplifier, built into it by means of an additional SiO_2 layer (100 nm) between the rectifying p^+ electrodes and the metallization (Al). Such an approach made it possible to avoid galvanic coupling of the detector to the charge-sensitive preamplifiers (see below). This is an essential feature in the case of integrated preamplifiers, since the spatial restrictions make it impossible to create large separating capacitances in an integrated circuit. In addition, each detecting element has an individual load resistor (3.2 MΩ) of polysilicon. In contrast to the traditional planar technology, which uses ion implantation, the rectifying and ohmic electrodes are obtained by means of boron and phosphorous diffusion, respectively. The strips (512) of width 10 μm and length 23 mm are arranged with pitch 25 μm on an n-Si wafer of thickness 260 μm. The mean leakage current at the voltage of complete depletion (100 V in this example) was 90 nA/strip. The spatial resolution achieved by such a detector is $\sigma=3.5$ μm. Microstrip detectors with built-in separating capacitances and load resistors are currently becoming more and more popular (see, for example, Refs. 45 and 74).

In a number of problems, particularly for the detection of γ and x rays, the preferred material for the detectors is single-crystal germanium. In contrast to silicon detectors, germanium detectors must necessarily be cooled to liquid-nitrogen temperatures. Microstrip detectors made from high-purity n-type germanium (HP Ge) were developed for use as part of an active target in a measurement of the particle multiplicity in photoproduction experiments at CERN.[38] The detectors (Fig. 6a) had 48 strips (width 50 μm, pitch 100 μm) and 96 strips (width 25 μm, pitch 50 μm) on plates of HP Ge of thickness 5 mm. A Pd (0.03 μm)–Au (1.25 μm) layer was used as a mask during the fabrication of the strip structure. The detectors had reverse currents 10^{-10} A at the voltage of complete depletion 500 V.

Single-coordinate (minimal pitch 200 μm) and two-coordinate (minimal pitch 1 mm) MSDs of HP Ge (Fig. 6b), fabricated by the firm Intertechnique using an original photomasking technology, were demonstrated in Ref. 39. This technology makes it possible to obtain strip structures

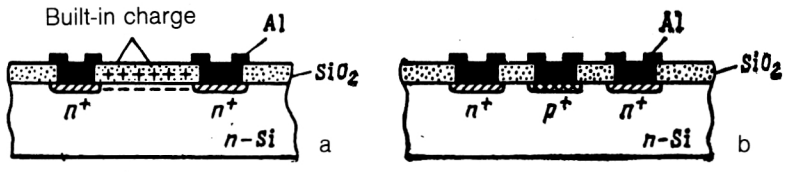

FIG. 7. Illustration of the problem of short-circuiting of strips in a two-coordinate MSD (a) and its solution by the introduction of separating floating p^+ strips (b).

TABLE I. Silicon MSDs fabricated by Intertechnique.

Type	Number of strips	Strip width, μm	Pitch, μm	Working surface, mm^2
IPS 50 × 50-300-N12	12	4000	4200	50×50
IPS 42 × 50-300-N24	24	2000	2100	42×50
IPS 12 × 51-300-N64	64	400	800	12×51
IPS 50 × 50-300-N250	250	100	200	50×50
IPS 26 × 26-300-N520	520	18	50	26×26

of any geometrical configuration, keeping the total reverse current at the level of tenths of a nanoampere in detectors measuring 40×40×15 mm. It should be said that the production of germanium MSDs is a complicated technological task requiring high methodological skill.

Two-coordinate MSDs (with two-sided readout from orthogonally arranged strips) using the standard planar method encounter the problem of built-in positive charge at the Si–SiO_2 interface.[40] This charge induces an electron-accumulating layer, and this leads to shorting of neighboring n^+ strips. The problem was solved[41] by introducing separating "floating" p^+ strips between the information n^+ strips (Fig. 7). The separating strips effectively increased the resistance between the information strips (to 10 MΩ) without destroying the mechanism of capacitative division (see below). In the absence of the separating strips, the resistance was several kilo-ohms. The development in two-coordinate MSDs of the idea of creating built-in separating capacitances[37] led to the appearance of some original solutions, in particular the use, in place of n^+ strips, of sections of the surface that accumulate electrons.[42]

At the present time, several firms are capable of industrial fabrication of different types of silicon MSDs, for example, Intertechnique (France)[43] and Micron Semiconductor (Great Britain).[44] Microstrip detectors using HP Ge are fabricated by Intertechnique. Tables I–III give the parameters of the most typical MSDs manufactured by these firms. Microstrip detectors are also being developed and fabricated in our country, in particular at RNIIRP (Riga), JINR (Dubna), and the Leningrad Institute of Nuclear Physics.[45–47] The detectors have sizes up to 40 ×40 mm and strips with pitch 25–200 μm.

Readout from microstrip detectors. In a semiconductor detector, the information carrier is the charge Q_0 produced by a particle in the process of ionization in the sensitive volume. The reverse bias voltage U_b applied to the p–n junction makes it possible to collect electrons and holes at the corresponding electrodes of the detector. The signal pulse has a rise time determined by the time of charge collection, which depends on the carrier mobility μ [1350 $cm^2 \cdot V^{-1} \cdot sec^{-1}$ for electrons and 480 $cm^2 \cdot V^{-1} \cdot sec^{-1}$ for holes in silicon at 300 K], the thickness d of the depleted region, and the voltage U_b ($t \simeq d^2/\mu U_b$). The maximum collection time in an MSD ($d=300$ μm) for $U_b=100$ V is 10 and 25 nsec for the electrons and holes, respectively. For the detection of minimally ionizing particles, the signal rise time is shorter than the maximum collection time, since the charge is uniformly distributed over the thickness of the detector. Thus, the MSD has in principle a fast response.

The signals are usually read out by means of low-noise preamplifiers (PA), which have either dc or ac coupling to the MSD (Fig. 8). The use in the first case of low-noise current amplifiers with bipolar high-frequency transistors (see, for example, Ref. 36) makes it possible to optimize the readout time of the MSD and ensures the best shielding from interference due to the low input impedance of the preamplifiers and lower (compared with charge-sensitive preamplifiers) dissipated power, this being a factor of no small importance, given the appreciable number of information outputs of the MSD. However, such an arrangement requires conditions under which the reverse currents of the detector strips are so small that they do not change the regime of operation of the input transistor of the preamplifier. Moreover, the occurrence of breakdown on a

TABLE II. Microstrip detectors fabricated by Micron Semiconductor.

Type	Number of strips	Number of information strips	Strip width, μm	Pitch, μm	Working surface, mm^2
MS F	25	25	1975	2000	50×50
MS V	256	256	250	300	77×57
MS B	1000	1000	25	50	50×50
MS C	1000	296	40	50	50×50
MS N	701	176	40	50	91×35
DS O	512	512	5	25 (N) 50 (P)	60×32

Note: The DS O is a two-coordinate MSD having 256 strips on each side.

TABLE III. Germanium MSDs fabricated by Intertechnique.

Type	Working surface, mm^2	Thickness, mm	Number of strips		Pitch, μm
			X	Y	
EGPS 10×10—0,5 N20	10×10	0,5	20	—	500
EGPS 40×40—3 N200	40×40	3	200	—	200
EGPS 45×45—15 N20×20	50×50	15	5	5	10 000
EGPS 40×40—10 N20×20	40×40	10	20	20	2 000

strip can lead to failure of the entire preamplifier. Therefore, at the present time one generally uses ac connection of charge-sensitive preamplifiers to the MSD. This fact is also reflected in the technological solutions (as was shown above) in the development of strip structures with built-in separating capacitances.[37,45,74]

Depending on the spatial and double-particle resolutions required by the experiment and on the possibilities of realizing the readout system, various methods of signal readout are used in MSDs (Fig. 9).

1. Parallel readout of signals from each strip. This method realizes the best readout time and best attainable double-particle resolution. The problem is the large number of readout outputs for detectors with high discreteness (strip pitch 10–25 μm).

2. Parallel readout with pitch of readout outputs greater than the pitch of the strips (see outputs 1 and 2 in Fig. 9) using the method of charge division on regular capacitance structures that are MSDs.[48] The interstrip capacitance must be appreciably greater than the capacitance of an individual strip ($C_b \gg C_s$). The strips from which there is no signal readout are called floating strips. Note that a bias voltage arises on the floating strip because there is a certain conductivity in the interstrip region. The maximum interval between the signal strips is limited by the signal-to-noise ratio. As a rule, for strip pitch 10–25 μm, the strip interval is not more than 4–5 strip pitches. It is necessary to have a signal-to-noise ratio $Q_0/\sigma_n \geqslant 15$ if one wishes to distinguish a signal from the floating strips at the level $3\sigma_n$. Capacitative division makes it possible to reduce the number of information outputs (by 2–4 times) without significant lowering of the spatial resolution. A shortcoming of the method is the lowering of the double-particle resolution compared with readout from each strip.

3. Readout using resistive charge division between strips (see outputs 2 and 3 in Fig. 9).[49] In this case, the MSD can be represented in the form of distributed RC structures like continuous STDs (see Sec. 1). The resistive layer can be formed either by incomplete depletion of the surface layer[50,51] or by depositing a special resistive covering between strips. Resistive division makes it possible to reduce the number of signal outputs, but for a number of reasons is not widely used, in particular, because of the additional noise contribution of the interstrip resistor and the longer readout time compared with other readout methods.

Spatial resolution. The main purpose of MSDs, responsible for their development, is the detection of relativistic (minimally ionizing) particles. In this case, the charge produced in the process of ionization is uniformly distributed along the track over the complete thickness of the MSD. The limiting spatial resolution of the detector is determined by the dimensions of the region of the transverse distribution of the charge (we assume that the particle passes along the normal to the plane of the detector). Electrons released by the ionization process have a very short range in silicon (the energy of most of them is less than 10 keV), and the standard deviation of the transverse charge distribution is approximately 1 μm.[6] It should be mentioned that the "tail" of the distribution due to energetic δ electrons may reach 5 μm.

The most probable energy losses in an MSD are determined by the Landau distribution and in silicon are 29 keV for silicon of thickness 100 μm.[52] Thus, in an MSD of thickness $\simeq 300$ μm the number of induced electron–hole pairs is 2.4×10^4, i.e., the charge is of order 4×10^{-15} C.

As the charge is collected, the spatial distribution becomes broader because of the diffusion of the carriers and their mutual repulsion. The standard deviation σ of the spatial distribution reaches 5 μm for the holes and 8 μm for the electrons for collection thickness 300 μm.[7]

For strip pitch exceeding 50 μm, the charge from a

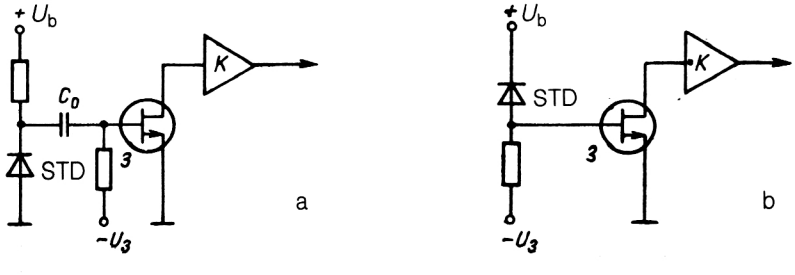

FIG. 8. Detector–preamplifier switching circuits: a) ac; b) dc.

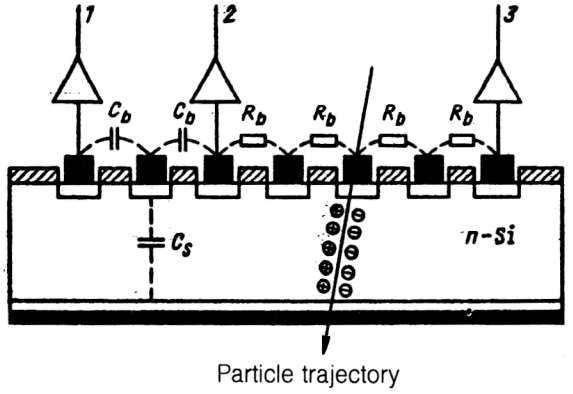

FIG. 9. Methods of data readout from a microstrip detector (channels *1* and *2* use capacitative division; channels *2* and *3*, resistive division).

normally incident particle is collected on one strip. In this case, the spatial resolution of the MSD is determined solely by the strip pitch:

$$\sigma = S/\sqrt{12}.$$

For MSDs with strip pitch 25 μm, charge is collected on several strips. The distribution of the charge (and, accordingly, the pulse heights of the readout signals) over the strips determines the concept of a "cluster." Figure 10 shows the distributions of the pulse heights in a cluster (a) and the probability of the number of strips forming a cluster for an MSD with pitch 25 μm (b).[53] It can be seen that collection of charge on two strips is the most probable.

The formation of clusters permits determination of the position by the method of searching for the centroid of the pulse-height distribution,[49,54] and a spatial resolution σ better than that given by the strip pitch can be obtained. In this case, the resolution is essentially determined solely by the signal-to-noise ratio:

$$\alpha = \alpha S \sigma_n Q_0,$$

where α is a constant that depends on the method used to calculate the pulse-height distribution. For three-strip clusters, $\alpha = 2$ (Ref. 5). As an example of the use of centroid search in MSDs we can mention the achievement in Ref. 54 of $\sigma = 3$ μm for detectors with strip pitch 20 μm ($S/\sqrt{12} = 5.8$ μm). The use of centroid search under conditions of capacitative division with readout from every third strip (readout interval 60 μm) makes it possible to achieve a resolution of $\sigma = 4.5$ μm, and in the case of readout from every sixth strip (interval 120 μm) resolution 8.7 μm.[55]

As we have already said, the use of resistive division is less favorable because of the poorer signal-to-noise ratio. It is expedient to use resistive division if it is possible to increase the signal that is read out. This happens if the thickness of the detector is increased or one is detecting particles for which the energy release in the detector is appreciably greater than for minimally ionizing particles. Thus, in a detector of thickness 900 μm using resistive division a resolution of $\sigma = 22$ μm was achieved with an intrastrip gap of 330 μm for detection of charged particles with energy 140 GeV (from calculations a resolution 18–19 μm was expected).[51] Note that, in contrast to the interstrip region, the resolution in the region of a strip will be determined solely by the strip width, $\sigma = W\sqrt{12}$.

Let us now consider how the ratio of the strip width W to the interstrip spacing b influences the characteristics of MSDs. The detailed investigation presented in Ref. 56 enables us to state that for minimally ionizing particles the spatial resolution is determined solely by the strip pitch S. At the same time, it is preferable to make the interstrip separation as large as possible, i.e., to have strips as thin as the technology permits. Such an approach leads, on the one hand, to a reduction of the interstrip capacitance and, therefore, to a decrease in the mutual electrical interference between the signal outputs and, on the other hand, to a decrease of the capacitance of the strips and, accordingly, the noise level. A certain problem with a large interstrip separation may be the appearance of surface effects, namely, additional leakage currents and centers of recombination and capture of charges. If the detectors are used for strongly ionizing, short-range particles, which produce large numbers of electron–hole pairs in the surface region of the MSDs, the holes (moving to the collecting electrodes) recombine with electrons on the surface. The built-in positive charge at the SiO_2–Si interface that accumulates the electrons increases this possibility. For example, if α particles are incident in the interstrip gap, this leads to the appearance of a satellite peak,[56] and with increasing interstrip separation this is displaced from the main peak in the low-energy direction and becomes broader.

Besides the use of MSDs in high-energy physics, we should also mention the prospects for using them to detect particles of low and intermediate energies. The good spec-

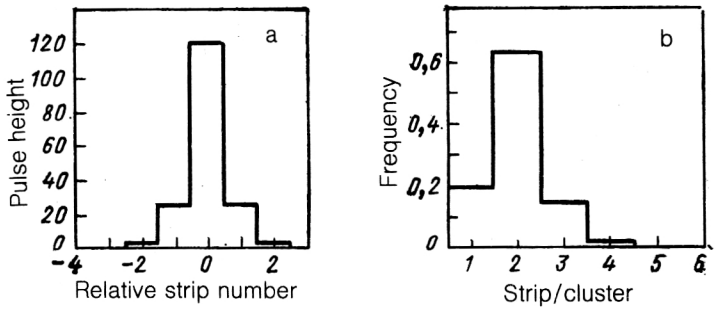

FIG. 10. Properties of clusters in a microstrip detector with pitch 25 μm.

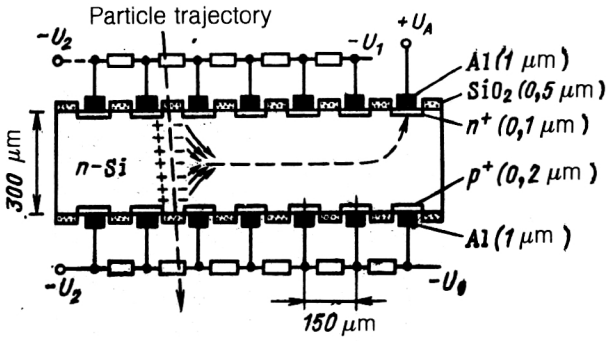

FIG. 11. Structure of a semiconductor drift chamber.

trometric properties of MSDs make it possible to obtain for such particles fairly complete information about the position, energy, and specific losses and, thus, provide identification possibilities.[57]

Semiconductor drift chambers

The search for ways to reduce the number of readout outputs in miniaturized track detectors led to the development of a device that has become known as a semiconductor drift chamber (SDC).

The idea of the SDC is to use a new principle for collecting charge in a semiconductor under the influence of two independent electric fields in the volume of a detector,[58] namely, the field that creates the depletion and a field that realizes directed drift of the carriers parallel to the surface of the device.

Figure 11 is a simplified scheme of an SDC. The substrate is high-resistivity n-type silicon. Planar technology analogous to the fabrication of microstrip detectors is used. The thickness of the substrate is 300 μm, determined as in the case of MSDs by the necessary magnitude of the signal from minimally ionizing particles. On both sides of the substrate, rectifying contacts (p^+) are created in the form of strips. Complete depletion is achieved through an n^+ contact, which plays the part of a readout anode. The design exploits the possibility of combining a fairly large semiconductor substrate (of order 1 cm^2) with low capacitance of the n^+ contact (a few picofarads). It is important that depletion is achieved by a voltage four times lower than for an MSD of the same thickness.

In the central region of the working volume, a minimum of the potential for the majority carriers (electrons) is produced. The potential of the longitudinal drift field in the SDC is produced by a linearly rising potential applied to the p^+ strips. Figure 12 shows the distribution of the potentials calculated for the superposition of the electric fields in the volume of an SDC.[59] The existence of a region of potential minimum for the majority carriers is the distinctive feature of the SDCs. It should be mentioned that they require a rather high uniformity of the material in the longitudinal direction in order to obtain a constant or monotonically varying drift velocity. Above all, this is necessary in order to realize simple and accurate calibration.

Readout from semiconductor drift chambers. The charge is collected in SDCs as follows. Electrons released by the process of ionization as a particle passes drift at the first instant, under the influence of the transverse field, into the region of the potential minimum (central part of the detector), their self-field being screened by the p^+–n junction. The time of drift of the electrons to the central region is a few nanoseconds. Then, under the influence of the longitudinal field gradient, the electrons drift along the surface of the substrate to the readout n^+ electrode. The drift dynamics of electrons in SDCs was considered in detail in Ref. 60. The time between the passage of an ionizing particle and the appearance of a signal at the anode, due to the finite drift velocity of the electrons, is proportional to the distance between the position at which the ionizing particle passes and the n^+ electrode (as in an ordinary gas drift chamber) and yields the position information.

Since the position information in SDCs is determined by the time of delay of the arrival of the electrons at the readout electrode, in the ideal case (if diffusion of the electrons and the influence of their mutual repulsion is ignored) one can assume that the component of the electron drift velocity in the direction of the readout electrode does not depend on the position at which the electrons are pro-

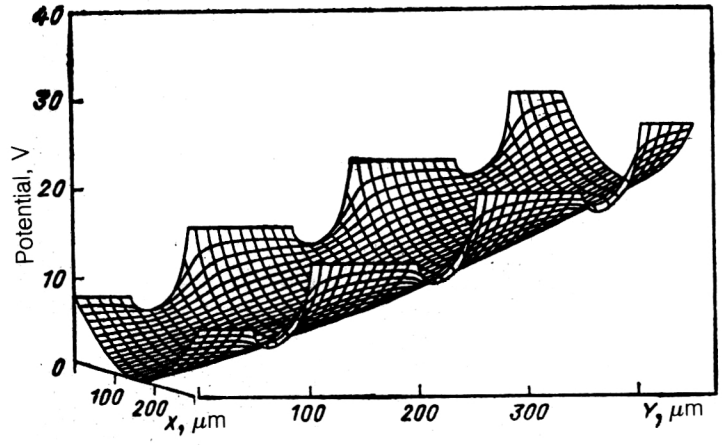

FIG. 12. Distribution of electric field within a semiconductor drift chamber.[59]

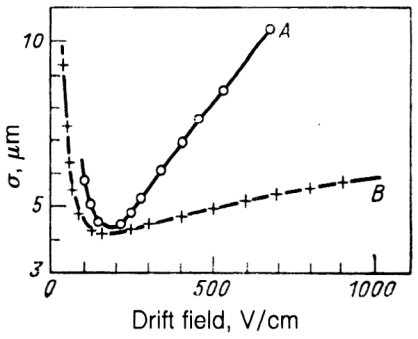

FIG. 13. Dependence of spatial resolution of SDC on the drift field.[59]

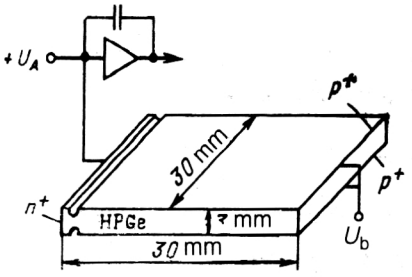

FIG. 14. Structure of an HP Ge semiconductor drift chamber.[62]

duced in the track. The electrons produced by the ionization process must reach the readout electrode practically simultaneously, giving a sharp peak, the height of which is determined by the ionization losses, while the position of the maximum on the time axis is determined by the position of the particle. If the time of arrival of the ionizing particle and the electron drift velocity in the semiconductor are known, the coordinate can be obtained from measurement of the time of appearance of the peak. The drift velocity is in the range 1–10 μm/nsec. The transverse drift of the electrons and their mutual repulsion, which increase the spatial region of the collected charge, and also the leakage currents of the detector and the noise of the readout electronics lead to uncertainties in the determination of the coordinate.

The influence of the carrier dynamics on the output pulse can be reduced by increasing the drift velocity, i.e., by increasing the strength of the longitudinal field. The maximal drift field that is in practice possible in the case of planar technology is 300 V/mm.[60]

Spatial resolution. The problem of the influence of electronic noise on the determination of the time mark of the signal of a semiconductor detector is fairly well known in nuclear spectroscopy. A traditional method is to use a linear filter that optimizes the parameters of the output signal in order to determine the arrival time from the crossing of a threshold. The optimum signal processing for a semiconductor drift chamber thus consists of realizing a linear filter that minimizes the fluctuations in the time of crossing of the threshold.

The results of measurements made with semiconductor drift chambers (thickness 300 μm, pitch 150 μm of the p^+ strips, drift gap 4 mm) are shown in Fig. 13, which is taken from Ref. 59. The signal was excited by a beam (of diameter 20 μm) of infrared light from a GaAs light-emitting diode. The pulse intensity was chosen in order to generate about 24 000 electron–hole pairs (corresponding to a minimally ionizing particle passing through Si of thickness 300 μm). The measurements were made for different drift fields with the same filter, which was ideal only for a field of 130 V/cm (curve A). Curve B (the result of a calculation) shows the behavior of the spatial accuracy if optimal filtering is chosen for each drift field. Investigations of this SDC under real conditions using a beam of π^- mesons (100 GeV/c) from the SPS accelerator at CERN gave $\sigma = 11$ μm.

Subdivision of the SDC anode into individual output cells makes it possible to organize a two-coordinate data readout. An anode of this type, segmented into 41 elements,[59] made it possible to obtain a two-coordinate resolution of $\sigma_{x,y} = 18 \times 24$ μm in an SDC measuring 17×11 mm tested in a pion beam.

It is worth mentioning the development of a germanium detector ($30 \times 30 \times 3$ mm) based on the SDC principle (Fig. 14).[62] The drift field in it was produced by a gradient of electrically active impurities along an HP Ge crystal. The resulting spatial resolution was better than 0.5 mm. It is proposed to use such a device for γ tomography.[62]

We should mention that as yet SDCs have not been used in a real experiment as position detectors of relativistic particles. However, the idea of such devices has proved to be very fruitful for bringing forward several developments of special semiconductor detectors: low-capacitance (1.5 pF/cm^2) photodiodes possessing a record low level of noise compared with ordinary semiconductor detectors of the same area, combined dE/E detectors, new types of completely depleted CCD detectors, and more (details can be found in Refs. 64–67).

Detectors based on charge-coupled devices

Semiconductor charge-coupled devices (CCD) have been known[68] since 1970. They are based on a matrix of MIS (metal–insulator–semiconductor) structures, each element of which can act as a charge time trap. Applying appropriate control potentials, one can realize row-by-row charge readout. Different forms of CCDs (one- and two-dimensional, two-, three-, and virtual-phase, with surface and volume channel) have found wide applications as converters of images obtained in infrared, visible, ultraviolet, or x-ray radiation, and also as analog or digital memories.

The possibility of using CCDs as detectors of minimally ionizing particles was demonstrated[69] in 1980. Subsequent tests of a telescope made of CCD detectors in a beam of relativistic particles using the apparatus of experiment NA-32 at CERN[70] confirmed the high detection parameters of CCDs—the resulting spatial (two-coordinate) resolution was $\sigma = 5$ μm, and the double-particle resolution was 20 μm. The sensitive surface of an individual

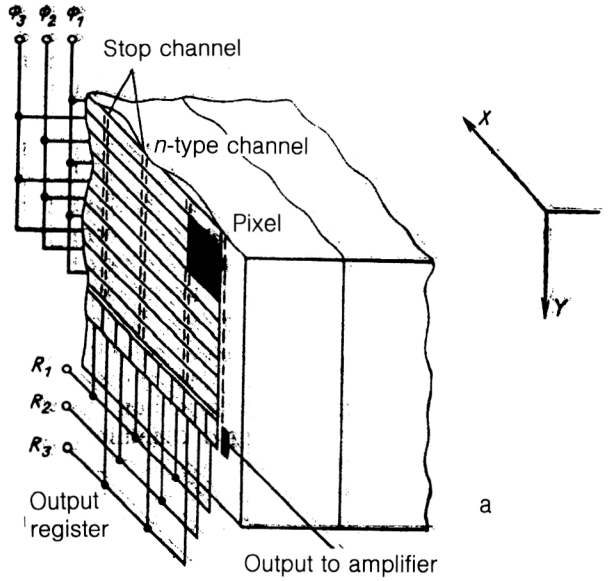

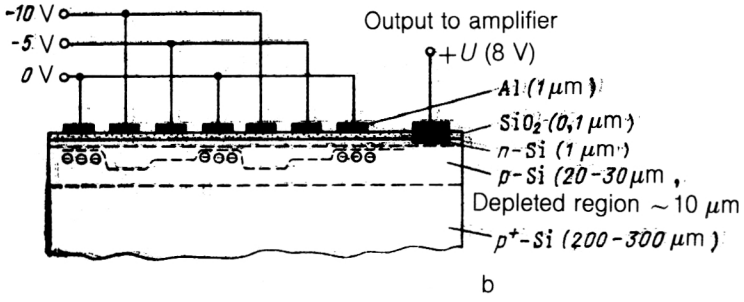

FIG. 15. General form (a) and section (b) of a standard CCD detector.

CCD measured 12.7×8.5 mm, and the total readout time was 75 msec. To obtain signal-to-noise ratios up to 20–30, the CCD detectors were cooled to 170 K.

Figure 15 shows the schematic form and section of the CCDs used in Ref. 70. They are based on a substrate of low-resistivity p-type silicon (10^{18}–10^{19} acceptors/cm^3) of thickness 300 μm with an epitaxial layer (10^{14} acceptors/cm^3) of about 25 μm. In the epitaxial layer an n-type channel (10^{16} donors/cm^3) with a thickness of about 1 μm is obtained by implantation. Rectangular electrodes were formed above the oxidized surface (SiO_2). Each triplet of electrodes forms a cell, a so-called pixel, measuring 22×22 μm. A positive potential is applied to the n-type channel, which has an ohmic contact, and, thus, a region depleted of charges is produced in the epitaxial layer.

The charge carriers (electrons) produced by an ionizing particle are collected in the n-type channel in regions of a minimum of the potential energy. Between the pixels, along the X axis, there are special built-in stopping channels in the form of implanted p-type regions, which prevent the movement of charge in the X direction. Along the Y axis, the pixels are electrically separated by barriers formed by controlling potentials Φ_1–Φ_3. The CCD detectors of this type are called three-phase devices with buried channel. The standard CCD detectors have an area of 1 cm^2, on which there are 10^5–10^6 pixels.

Data readout from CCD detectors. The charge readout from CCD detectors is realized (at a trigger signal command) by the successive application of synchronized potentials Φ_1, Φ_2, and Φ_3 to the gates with a definite tact frequency (see Fig. 15). If the sequence of potentials is changed by one tact (three phases), all charges of one row of pixels are displaced in Y by one pixel to the following row. From the lowest row of pixels, the charges are transmitted to a linear output structure—an output register R, in which, under the influence of analogous tact potentials R_1, R_2, R_3, the charges are shifted along the X axis to the output element. From the output element, signals are sent to the input of a low-noise amplifier, which is integrated onto the same substrate as the detector itself. After the information from the output register has been read, the information from the following row reaches it under the influence of the next tact (Φ_1,Φ_2,Φ_3). The time of the complete readout at frequency 1 MHz of the control potentials is tens of milliseconds.

Spatial resolution. Readout time. A distinctive feature of standard CCDs is the thin sensitive (depleted in carriers) region of 25 μm. For minimally ionizing particles, the charge Q_0 formed in an ionization process in a CCD detector is on the average 2000 electrons. The transverse diffusion and mutual repulsion in the process of collection lead to a broadening of the region over which the charge is distributed, and the charge reaches several pixels, usually four.[69] A further process that controls the pulse height of the signal and the width of the distribution is diffusion of carriers from part of the undepleted region. Figure 16

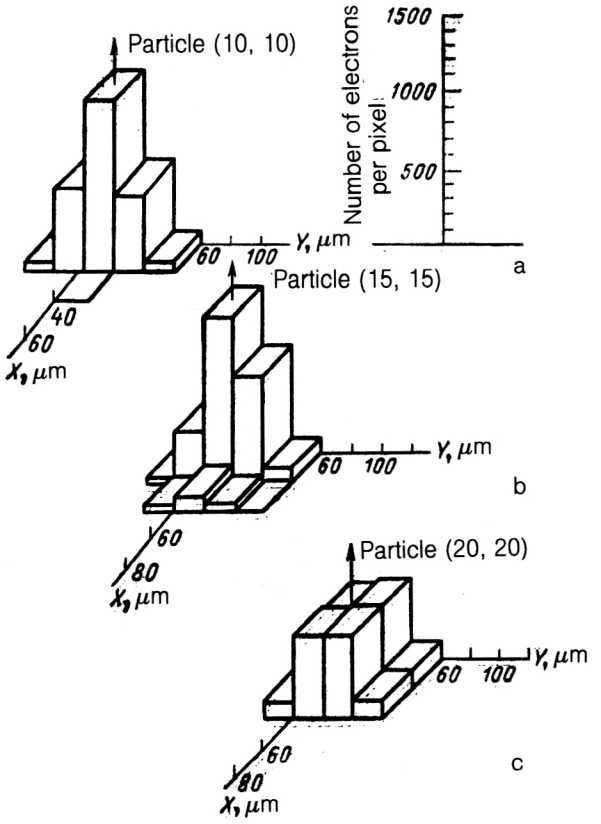

FIG. 16. Distribution of charge over pixels in a cluster for different coordinates (X,Y) of the particle track: a) the particle passed through the center of a pixel; b) and c) the particle passed closer to one of the edges of a pixel.[70]

shows the results of a simulation of the charge distribution on neighboring pixels (formation of a cluster) for three different coordinates of the track along which the particle passed through a pixel.[70] The distribution of the charge over several pixels makes it possible to use the method of finding the centroid of the distribution and, thus, to obtain a better spatial resolution than that determined by the separation of the pixels.

Figure 17 illustrates the expected spatial resolution (using the method of centroid search) as a function of the noise level. Cooling of the CCD to 120–170 °K, the low capacitance of the output element of the CCD (about 0.2 pF), and the use of the principle of correlated double sampling (see, for example, Ref. 71) in the amplifier integrated into the CCD make it possible to achieve a noise level of $\sigma_n = 30$–50 electron/pixel for readout at a frequency of order 1 MHz.[70,72]

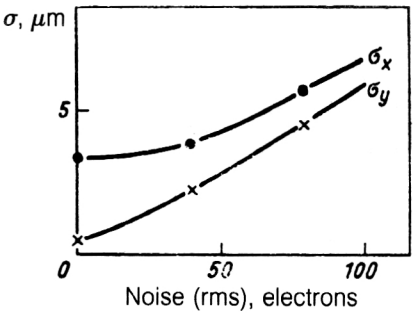

FIG. 17. Dependence of the spatial resolution of a CCD detector on the noise level.[70]

The possibility of using a standard CCD as a particle detector working at frequency 7.16 MHz at room temperature was demonstrated in Ref. 73. The noise level was $\sigma_n = 87$ electron/pixel.

A spatial resolution $\sigma < 5$ μm and double-particle resolution 20–40 μm are realized for particles detected by the CCD detector as a result of response to a trigger signal. The problem arises of excluding signals from particles that pass through the detector before the trigger or during the readout time. In the absence of control potentials, the former signals decay as a result of diffusion along the n-type channel with a characteristic time of 500 nsec. Figure 18 illustrates this process. It can be seen that these clusters can be eliminated. In addition, in the absence of a trigger it is possible to realize fast clearing of the detector with a frequency of order 10 MHz. Particles that enter the detector during the readout process can also be excluded, since they form very narrow (along the Y axis) clusters—in this case, the charge is distributed over one or two pixels.

The appreciable time required for signal readout from a CCD detector gives rise to an appreciable "dead" time of the experimental facility. Therefore, to obtain readout times adequate for typical electronic experiments it is necessary to develop CCD detectors that do not have just one output (as in standard optical CCD detectors) and divide the output register into several sections. If there is a division into 20 sections, the readout time becomes 4 msec.[69]

Completely depleted pn CCD detectors. In recent years, there has been intensive development of the method of completely depleted *pn* CCD detectors (see, for example, Refs. 64 and 66), which are based on the principle of semiconductor drift chambers.

Figure 19 gives a picture of the structure of such a detector. In a wafer of high-resistivity silicon ($\rho \geqslant 2$

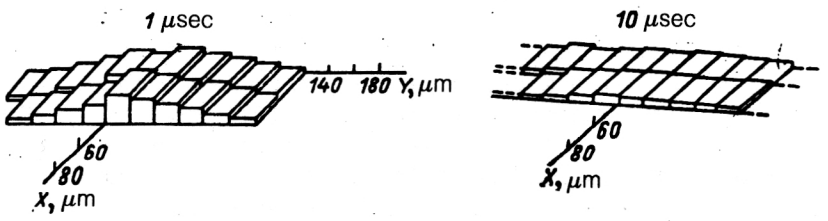

FIG. 18. Distribution of charge over pixels in a cluster at times 1 and 10 μsec after the particle has passed in the absence of control potentials (cf. Fig. 16).

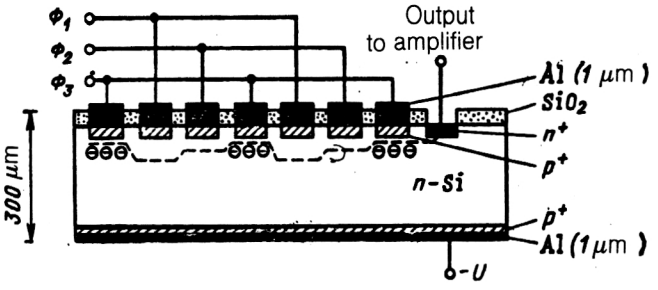

FIG. 19. Structure of a completely depleted *pn* CCD detector based on the drift-chamber principle.

kΩ·cm) of thickness 280 μm complete depletion is created by analogy with an SDC (as above) by means of continuous p^+ contacts and strip p^+ contacts, applied on opposite surfaces, and also an n^+ anode. Near the upper surface there is a potential minimum for electrons produced in the ionization process. Applying appropriate potentials (Φ_1, Φ_2, and Φ_3) to the shift registers, it is possible to create local minima of the potential. Variation of these potentials in time makes it possible to shift discretely the signal charge along the direction to the readout anode. Stop channels are formed at right angles to the shifting p^+ strips (by analogy with standard two-coordinate CCD detectors), these preventing the charge from flowing in the direction perpendicular to the plane of the figure. These stop channels are created by implantation of deep *n*-type regions. As was shown in Ref. 64, it is possible to obtain a signal-to-noise ratio of the order of 100 for *pn* CCD detectors working at room temperature and frequency 1 MHz.

Figure 20 shows the schematic form of a *pn* CCD detector developed for an astronomical x-ray telescope.[74] In the focal plane it is proposed to place a matrix of 12 such

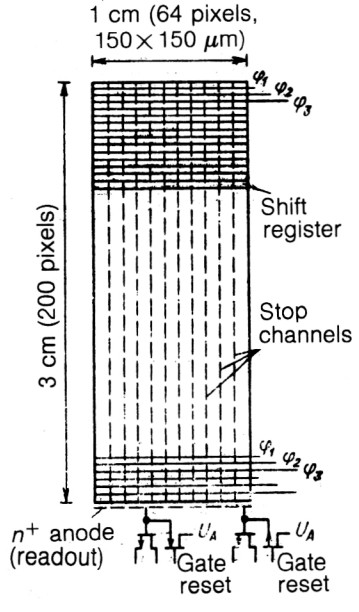

FIG. 20. Schematic form of a *pn* CCD detector developed for an astronomical x-ray telescope.[74]

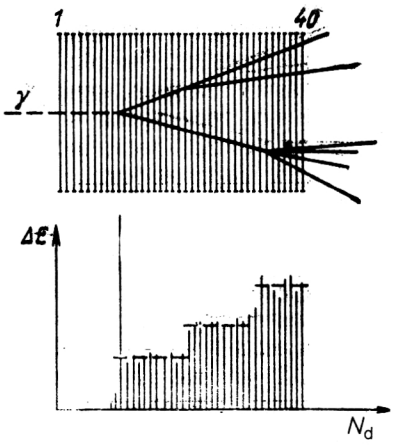

FIG. 21. Illustration of operation of a multicrystal telescope (40 Si detectors) as a multiplicity detector.[75]

pn CCD detectors, in each of which the thickness of the sensitive region is 280 μm. Each CCD (1×3 cm) has 64 ×200 pixels measuring 150×150 μm. The readout will be done by means of 64-output amplifiers in an integrated circuit (CAMEX 64; see Sec. 5).

4. MULTICRYSTAL TELESCOPE POSITION DEVICES

Multilayer telescope devices are used as position detectors to measure the longitudinal ionization density as a function of the coordinate along the beam direction and also to measure changes of the charge multiplicity.

Telescope detectors, which are often used as a so-called active target, consist of a set of thin silicon detectors having a thickness of about 300 μm and sensitive area up to 25 cm^2 packed closely in a module (the separation between the detectors is 100–200 μm). To reduce the detector capacitance, the sensitive region is segmented into parts (5–10).

Figure 21 shows an event with varying multiplicity detected by a multilayer silicon telescope (40 detectors) and its representation in the signals (ΔE) received from the individual layers (N_d).[75] A high-energy photon, passing through the first detectors without interaction, does not give rise to a signal, and at the output the detectors give an equivalent noise charge. In one of the detectors, the photon produces a pair of mesons—the interaction is characterized by a large energy deposition due to the recoil nuclei. The ionization losses of the two produced particles are measured by several detectors. Then, when the particles decay, there is a further jump in the signal amplitude (i.e., in the multiplicity), and so on along the entire telescope. The spatial resolution of telescope detectors is determined by the thickness of the layers of the sensitive region; for thickness 300 μm, $\sigma \simeq 100$ μm.

The development of discrete telescope detectors led to the construction of active continuous targets made of HP Ge (see Fig. 6),[38] in which strips play the part of individual detectors. The ionization density is detected as a function of the coordinate along the axis perpendicular to the

TABLE IV. Parameters of transistors for primary electronics.

Parameter	Bipolar	JFET	MOSFET
Limiting noise frequency, $1/f$, kHz	$\leqslant 1$	$\leqslant 1$	$\leqslant 1{\cdot}0$—1000
Equivalent voltage of thermal noise ($u/\sqrt{\text{Hz}}$, nV	1	<1	10
Current of drain (or collector), mA	0,2	5	10
Current of gate (or base), μA	1	10^{-3}	$<10^{-6}$
Pulse processing time, μsec	0,01—0,1	0,1—10	0,1—10

strips. A germanium volume detector has advantages with regard to the spatial resolution compared with silicon telescope detectors (approximately 50–100 μm along the beam direction); in addition, there is a gain in the signal pulse height due to the absence of gaps between the detectors and the large charge number of germanium.

Another application of multicrystal telescopes is their use as a first-level trigger. The layered structure makes it possible to determine jumps of the multiplicity from secondary interactions of the detectors and to realize a trigger in which the selection criterion is differences in the multiplicities detected by two telescopes of the detectors, as, for example, in Ref. 76.

5. ELECTRONICS FOR SEMICONDUCTOR TRACK DETECTORS

To obtain information from semiconductor track detectors, it is necessary to make a choice between the number of signal outputs and the finite time of obtaining the data. The product of the number of serial processing channels and the conversion time is constant for a given type of readout systems and is determined by the structure of the readout system, i.e., for the maximal number of outputs (parallel readout) we obtain the minimal processing time, while for the minimal number of outputs (serial readout) the processing time is maximal. To a large degree, this influenced the development of directly analog signal-processing channels as well as the actual structures of the readout systems. It became necessary to use methods of converting spectrometric information different from those traditionally applied in semiconductor spectrometry and also to take advantage of the latest advances in the technology of electronics.

The main functions of the systems of data readout from semiconductor track detectors are: amplification of the signals with the lowest possible noise before conversion and filtering of the analog signal (optimization of the signal-to-noise ratio); storage and multiplexing; analog-to-digital conversion.

The first two functions are implemented by the primary detector electronics.

A very important problem in the electronics for semiconductor track detectors is the power limitations which arise because of the small spatial region available for the primary detector electronics.

Input elements of primary electronics

Despite the significant differences in the principles of obtaining and analyzing data in the considered types of semiconductor track detectors, a characteristic common to all is the signal-to-noise ratio. This parameter determines the relationship between the detector proper and the subsequent readout and processing electronics. Thus, in microstrip detectors the signal-to-noise ratio determines the maximal interpolation factor or the signal-readout pitch; in detectors based on CCDs, it determines the maximal rate of signal transfer and, accordingly, the readout time; in semiconductor drift chambers, it governs the accuracy in the determination of the carrier drift time, etc. Thus, the achievement of a maximal signal-to-noise ratio is the most general task of the supporting electronics of semiconductor track detectors and can be considered independently of the type of detector and structure of the readout system.

At the present time, significant progress is being made in the development of special low-noise transistors for the primary detector electronics. Let us consider the main relationships for the noise characteristics of the transistors used as input elements of the readout electronics. The characteristics of the various types of transistors are given in Table IV.[77]

In the high-frequency region, thermal noise is predominant. The equivalent voltage of the thermal noise of bipolar transistors in the frequency interval Δf is determined by the equation

$$U_{\text{eq}} = \sqrt{4kT(r_b + 1/2h)\Delta f},$$

where h is the transfer coefficient of the transistor, and r_b is the resistance of the base.

For FET transistors, the equivalent noise voltage can be written as

$$U_{\text{eq}} = \sqrt{4kT(2/3)(1/g_m)\Delta f},$$

where $g_m = dI_d/dU_{gs}$ is the transconductance (I_d is the drain current of the transistor, U_{gs} is the gate-source voltage). For the MOSFET transistors, g_m is determined by the size of the elements of the device:

$$g_m \approx \sqrt{WI_d/t_{0x}L},$$

where W is the gate width, t_{0x} is the thickness of the oxide layer (which may be of order 50 nm), and L is the gate length.

In the low-frequency region, the equivalent noise signal for bipolar transistors is proportional to the base current and may be appreciable. The equivalent noise signal for FET transistors is proportional to the gate current and is insignificant.

Noise of the form $1/f$ mainly influences the dynamic characteristics of signal readout, and in our case is important only for MOSFET transistors. To improve these characteristics, one uses technologies in which one can reduce the spatial size of the semiconductor structures to microns.

Analysis shows that at the present time the requirements of operation as input elements are best met by FET transistors, which ensure the smallest noise contribution (in particular, JFET transistors). However, the decisive factor leading to the general use in detector electronics of MOSFET structures is their technological compatibility with the subsequent elements of the detector electronics. The FET transistors are actively used in both discrete and integrated circuits together with the analog part of the detector electronics. Silicon MOSFET transistors with spatial structures of about 0.5 μm, low noise, and $g_m = 60$ mA/V are described in Ref. 78. In principle, such transistors can be fabricated by the integrated technology, but the LSI (large-scale integration) technology required for this with spatial structures 0.2–0.5 μm has not yet reached the stage of experimental testing.

A detailed analysis of FET structures used as input elements of detector electronics can be found in Ref. 77.

We should mention the recent reports of the development of bipolar microwave transistors with very low base resistance ($r_b \simeq 15\ \Omega$), permitting effective use of them as input elements of detector electronics.[79] Semiconductor amplifying structures based on GaAs,[80] which can also withstand much higher radiation, are promising.

Amplification of signals. Basic relationships. The considered characteristics of the input elements of the primary detector electronics are fundamental for the amplification and optimal processing of charge signals and the creation of amplification circuits.

The initial signal amplification is based on three types of amplifying device: charge-sensitive, current, and voltage amplifier.[81]

Charge-sensitive preamplifiers, possessing a high input resistance and feedback resistance of order 1 GΩ, make it possible to reduce significantly the influence of noise sources. Another important feature of charge-sensitive devices is the possibility of obtaining a so-called cold resistance,[81] which has noise characteristics significantly better than those of the physical resistance. The processing time for the charge-sensitive device is determined by the input time constant, which may be quite small.

The current device of a preamplifier has a large noise signal compared with a charge-sensitive device, and this explains the need to increase the feedback resistor. However, for fast signals the noise conditions may be acceptable. Current preamplifiers have a short processing time.

Voltage amplifiers as preamplifiers are of interest when semiconductor detectors are used in the regime of complete depletion, when the capacitance of the detector can be assumed to be constant, and the charge signal can be directly integrated in the capacitor of the detector. A voltage amplifier has a high noise level compared with a charge-sensitive amplifier, but in such a device it is possible to achieve a short processing time even in the case of appreciable detector capacitances.

The rms value of the equivalent noise charge (ENC) of a charge-sensitive preamplifier for the series noise of a FET transistor and a semiconductor detector can be represented in the form

$$\mathrm{ENC}_s = 2\sqrt{2/3}(kTC_d)^{1/2}[(C_a/C_d)^{1/2} + (C_d/C_a)^{1/2}] \times (\tau_a/t_m)^{1/2}\xi_s,$$

where C_d and C_a are the capacitances of the detector and the preamplifier, $\tau_a = C_a/g_m$ is the time constant of the input element, g_m is the transconductance of the input element, t_m is the shaping time constant, and $\xi_s = (1 + R_{\mathrm{ext}}/R_s)^{1/2}$ is the white-noise component (R_s is the intrinsic resistance of the input element, the base resistance, or the gate resistance).

The expression in the square brackets is the optimizing factor that relates the detector and the preamplifier. In this case, the minimal equivalent noise (ENC) is ensured for $C_d = C_a$:

$$\mathrm{ENC}_{s\ \mathrm{opt}} = 4\sqrt{2/3}(kTC_d)^{1/2}(\tau_a/t_m)^{1/2}\xi_s.$$

It is obvious that for detectors with low capacitances this relation can be achieved.

The value of the time constant τ_a can be expressed in terms of the frequency band of the gain, the time of passage of the electrons through the channel, and the parameters of the output element. For FET transistors

$$\tau_a = C_a/g_m \approx 1/f_a \approx \mu_e W_0/L^2,$$

where μ_e is the electron mobility, W_0 is the potential, and L is the channel length.

The influence of sources of parallel noise (resistors, shunting detector and preamplifier input, and also the leakage current of the detector and the gate current) can be determined already with allowance for an optimal shaping time constant. Under the condition of equality of the series and the parallel equivalent noise ($\mathrm{ENC}_s = \mathrm{ENC}_p$), it is possible to obtain optimal relations for the shaping time constant:

$$t_{m\ \mathrm{opt}} = 4\tau_a^{1/2}(R_p C_a)^{1/2}\xi_s \quad \text{(for thermal noise)},$$

$$t_{m\ \mathrm{opt}} = 4\tau_a^{1/2}\left(2\frac{kT}{e}C_a/I_d\right)^{1/2}\xi_s$$

(for detector leakage currents).

For $t_m = t_{m\mathrm{opt}}$, the total equivalent noise charge signal satisfies $\mathrm{ENC}_{\min} = \sqrt{2}\mathrm{ENC}_s$. Thus, to eliminate the sources of parallel noise (lower the leakage current of the detector and eliminate resistance at the input), the equivalent noise charge must be reduced by a factor $\sqrt{2}$.

TABLE V. Estimates of equivalent noise charge.

Type of STD	CCD, SDC	MSD (of small area)	MSD
C_d, pF	0,1	1,0	30
ENC_{opt}, electrons	41	129	706

The corresponding series noise can be suppressed by increasing the shaping time constant t_m, but this reduces the load that can be carried and the time resolution of the preamplifiers.

The equivalent noise charge (ENC) for noise of the form $1/f$ depends strongly on the shaping time constant:

$$ENC_{1/f} \sim 2(A_f C_a)^{1/2} C_d^{1/2} [(C_a/C_d)^{1/2} + (C_d/C_a)^{1/2}]$$

and it is also minimized under the condition $C_d = C_a$:

$$ENC_{1/f\,opt} \sim 4(A_f C_a)^{1/2} C_d^{1/2},$$

where A_f and C_a are parameters that characterize the input element of the preamplifier and the shaping time constant.

Analysis of the relations for optimal amplification shows that the capacitance of the detector plays a significant part in the formation of the noise signal. The capacitance of a semiconductor strip detector is determined mainly by the spatial dimensions of the sensitive region and the technology used to fabricate the detector. For microstrip detectors (detector thickness about 300 μm) the capacitance at the preamplifier input (for primary detector electronics situated in the immediate vicinity of the detector) lies in the range 1–30 pF, depending on the size of the strips. For CCD detectors and semiconductor drift chambers, the capacitance C_d is approximately 0.1 pF and less. Estimates of the equivalent noise charge for these types of detectors with a charge-sensitive preamplifier for $\tau_a = C_a/g_m = 0.5$, $\xi_s = 1$, and $t_m = 50$ nsec are given in Table V.

A separate group, with much more complicated conditions of operation of the preamplifiers, is constituted by detectors with large area (semiconductor telescope detectors). The capacitance C_d of such detectors may reach 500 pF and more.

Multichannel integrated primary electronics

In the design of the readout structure, in order to reduce to a minimum the number of information outputs to the subsequent processing system, use is made of parallel storage of analog signals from each detector output and multiplexing for organization of serial or group readout of signals.[82]

Multichannel primary electronics for semiconductor track detectors has many important features, but the most important are the limitation on the space available for the detector electronics and, accordingly, the restrictions on the dissipated power. These conditions make it necessary to use the integrated technology for fabricating the primary detector electronics and to implement the signal-processing functions on the basis of principles corresponding to that technology.

The best known detector electronics for microstrip detectors is the integrated circuit MICROPLEX, which was first developed in the framework of the DELPHI project.[83] The integrated circuit contains 128 amplifying channels with parallel analog memory and serial readout. The size of the integrated circuit is 6.3×4.6 mm, and the pitch of the readout outputs is 50 μm. Figure 22 shows the circuit of the MICROPLEX readout channels. The initial processing is done by a charge-sensitive preamplifier (CSA) with discharge switch in a feedback. The need to use integrated technology led to the abandonment of the traditional methods of signal filtering on the basis of *RC–CR* circuits, since their realization in integrated technology is very complicated. In the given case, the filtering of the signals (optimization of the signal-to-noise ratio) is done with a time-variant filter using the integrating properties of

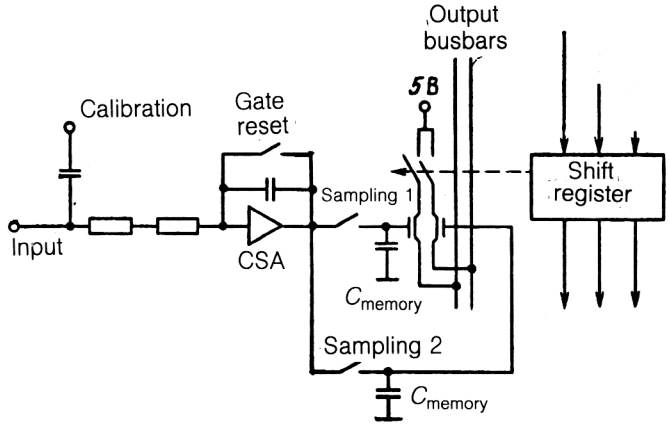

FIG. 22. Functional circuit of MICROPLEX readout channels.

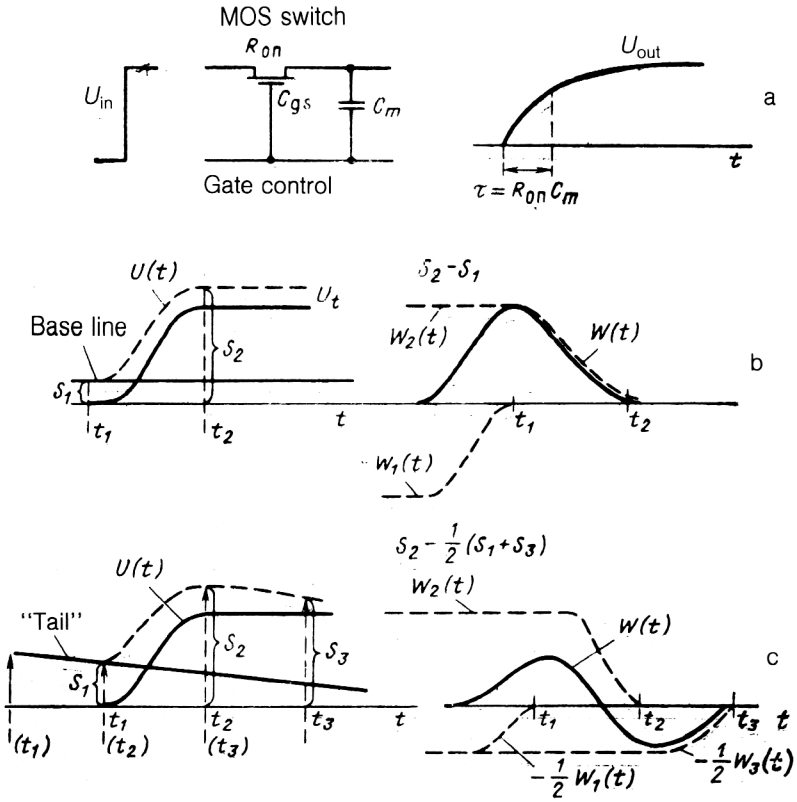

FIG. 23. Time-variant filters (sampling, storage, and multiplexing): a) operation of simplest time-variant filter; b) and c) shape of signal $U(t)$ and weight function $W(t)$ for the case of double and triple sampling, respectively [the weight function is determined by the sampling intervals $t_2 - t_1$ and $t_3 - t_2$, and also by the response of the amplifier with allowance for integration of the signals in the elements $R_{0n}C_m$ (Ref. 5)].

analog-memory capacitors (see, for example, Refs. 71 and 84).

The simplest time-variant filter is a circuit consisting of a transistor switch and a storage capacitor (Fig. 23a). The charge injected through the gate capacitance C_{gs} is optimized by a transistor with large input resistance and analog-memory capacitor. With respect to the injected charge, the charge of the analog memory (sampling) is proportional to the time constant $\tau = R_{0n}C_m$. For FET transistors, the time constant is inversely proportional to the limiting frequency of the transfer coefficient and can be tens or hundreds of picoseconds. An advantage of this scheme is the known signal readout time. The use of several correlated signal samplings (in several storage capacitors) makes it possible to realize weight functions of signal processing analogous to the traditional filters based on *RC–CR* circuits or delay-line filters. Figures 23b and 23c show the signals and form of the weight functions of time-variant filters. In the MICROPLEX scheme, time-variant filters with double correlated sampling are realized, while in the later developments there is triple correlated signal sampling. The equivalent noise charge was ENC=350 + $100C_d$ (ENC in electrons, C_d in picofarads).

The MICROPLEX readout regime is serial using an analog multiplexer and 128-bit control register. The signal readout frequency is of order 10^5 Hz.

The MICROPLEX device is fabricated using the 5 μm NMOS technology, and the required power is about 17 mW per channel. The main characteristics of the MICROPLEX device are given in Table VI. A defect of MICROPLEX is its relatively large dissipated power, this being due to the technology employed.

A development of integrated structure of detector electronics is represented by the microcircuits MX1, MX2, MX3, SVXIC[85,86] based on the 3-μm CMOS technology. This technology makes it possible to improve the characteristics of the readout detector electronics. The required power is significantly reduced, a high gain is obtained, and the required power can be regulated by an external applied voltage. The main characteristics of the MX3 and SCXIC microcircuits are given in Table VI.

The integrated circuit CAMEX, developed in the framework of the ALEPH project,[87] is a successful development of microchannel detector electronics for microstrip detectors. The main requirements in its development were the reduction of the dissipated power, minimization of the noise, and maximal rate of transmission to a low-resistance line. The 3-μm CMOS technology was used as a basis. In the initial stage, the integrated circuit of a charge-sensitive amplifier with a transmitter to a cable (50 Ω) was developed. Subsequently, the 60-channel integrated circuit DCPLEX with a time-variant filter with double correlated sampling, parallel storage of the analog signal, and serial readout was developed.[87] The desire to optimize as far as possible the process of conversion of the analog signal, in particular the signal-to-noise ratio, provided the stimulus for the development of a new circuit of the time-variant filter on the basis of the correlated samplings used in the CAMEX circuit.[88] The circuit of the CAMEX readout channel is shown in Fig. 24. The initial conversion is made by a charge-sensitive amplifier with a reset switch in a feedback: CSA1. The second amplifier CSA2 together with

TABLE VI. Parameters of integrated circuits of primary electronics.

Parameter	MICROPLEX	MX3	SVX IC	CAMEX	AMPLEX
Number of readout outputs	128	128	128	64	16
Range of input signals (fC)	0—200	0—200	0—100	0—100	0—200
Signal rise time, nsec	15	200	200	70	700
Effective input capacitance, pF	25	50	50	200	100
Noise (ENC rms), electrons (C in pF)	$350+100\,C_d$	$600+50C_d$	$200+80C_d$	$300+50C_d$	1000 (for $C_d=20$ pF)
Linearity, %	1	5	1	2	2
Readout time for one output, nsec	500	200	1000	330	1000
Dissipated power, mW	3000	70	150	120	20
Size of microcircuit, mm	6,4×4,5	6,28×6,86	6,4×4,2	6.35×4.95	4,1×4
Technology	NMOS (5 μm)	CMOS (3 μm)	CMOS (3 μm)	CMOS (3 μm)	CMOS (3 μm)

the storage capacitors C_1–C_4, switches S_1–S_4, and switch S_5 in a feedback realize a time-variant filter with fourfold sampling.

For a definite sequence of switching of the switches S_1–S_4 and S_5, it is possible to obtain at the CSA2 output a 4-fold signal and $\sqrt{4}$-fold noise. The signal-to-noise ratio is improved by 2 times. The equivalent noise signal obtained for this integrated circuit was

$$\mathrm{ENC}=300+50C_d,$$

where ENC is measured in electrons and C_d in picofarads.

At the present time, the integrated circuit CAMEX is realized in 64-channel form for microstrip detectors with readout pitch 100 μm with storage and serial readout of the channels (there is a 128-channel version for pitch 50 μm). The circuit measures 6.35×78 mm. The power released is 1.6 mW per channel. The basic properties of the CAMEX integrated circuit are given in Table VI.

Also of interest are the recent developments of multichannel readout electronics for semiconductor track detectors whose elements have a fairly high capacitance (of order 100 pF). An example is provided by the AMPLEX microcircuit,[89] which is realized on the basis of traditional methods of processing of signals from semiconductor detectors. The circuit is shown in Fig. 25. The input amplifier is a charge-sensitive preamplifier with a reset switch in a feedback. The filtering amplifier is realized in accordance with the traditional circuit of a time-variant filter, which realizes pseudo-Gaussian signal shaping. The readout is serial with storage in an analog memory. The number of channels is 16. The main characteristics of the AMPLEX circuit are given in Table VI. At the present time, attempts are being made to include the readout electronics directly in the structure of the detector.[90]

It is obvious that for operation with high loads it is desirable in microstrip detectors to have parallel readout without storing and multiplexing. An example of such fast readout electronics in the integrated technology is provided by the circuit developed for the microstrip detectors of the CDF experiment at FNAL.[91] In it, 128 channels of current amplifiers are integrated.

The development of the readout electronics for detectors based on CCDs does not present such complications as for microstrip detectors, since these detectors directly realize the possibility of serial readout of signals and give a much lower input capacitance. An example of readout electronics for CCD detectors is the circuit described in Ref. 69.

As we noted above, the readout electronics for semiconductor drift detectors differs fundamentally from the electronics for the microstrip and CCD detectors, since the information signal in the drift chambers is the pulse arrival time. Such electronics has been fairly widely investigated

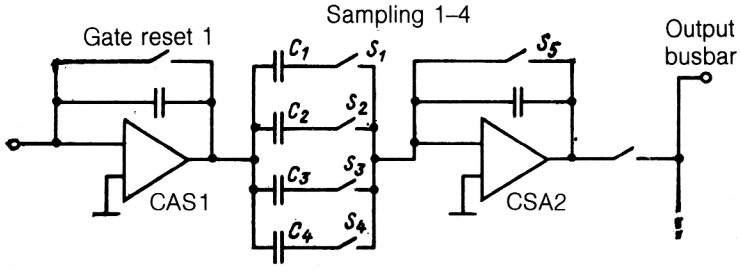

FIG. 24. Circuit of CAMEX readout channels.

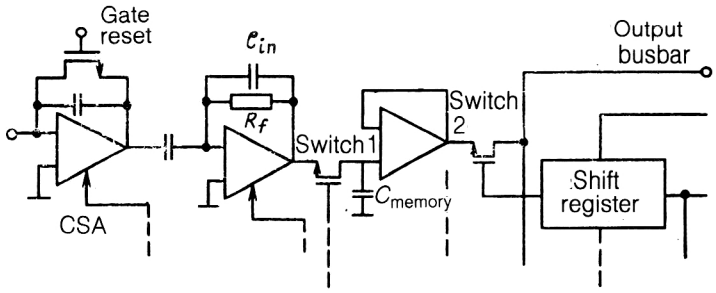

FIG. 25. Circuit of AMPLEX readout output.

and is extensively used in time measurements (see, for example, Ref. 92).

6. DEPENDENCE OF PARAMETERS OF SEMICONDUCTOR TRACK DETECTORS ON EXTERNAL CONDITIONS

For semiconductor detectors, an important condition for maintaining stability of their characteristics during long use is a clean surface. Since high-purity semiconductor materials have a tendency to capture molecules (oxygen, ions of heavy metals or organic compounds) from the environment, this can change the surface conductivity of the detectors. For this reason, various methods are used in the production of semiconductor detectors to shield the p–n junction: passivation of the surface by means of silicon oxides, deposition of insulating layers, for example, Si_3N_4, Al_2O_3, etc. It is obvious that operation of semiconductor detectors in an inert medium or in vacuum is preferable.

Influence of magnetic fields

One of the advantages of the semiconductor detectors used to measure the energy of particles is the insensitivity to the influence of magnetic fields. However, in the case of miniaturized semiconductor track detectors (especially microstrip detectors), it is necessary to take into account the influence of the magnetic field on the accuracy with which the position information is obtained. If the strength of the field (applied parallel to the strips) is a few teslas, the Lorentz force can displace the carriers by more than 10 μm.

The processes of charge collection in microstrip detectors under conditions of a magnetic field were investigated for a detector of thickness 280 μm with strips of width 20 μm and pitch 40 μm.[54] Readout was done from each strip. The magnetic field was oriented parallel to the horizontally placed strips and perpendicular to the beam of detected particles (200 GeV/c). The effects of collection of the hole and electron components of the charge were investigated.

Figure 26 shows the influence of the magnetic field on the charge distribution in the microstrip detector. In the absence of the field, the distribution is symmetric with FWHM=6 μm for a voltage $U=120$ V on the detector and with FWHC=4.5 μm at $U=200$ V (the distribution agrees with the theoretical distribution). The magnetic field gives rise to a drift of the charges in a direction that makes an angle Θ_L with the direction of the electric field in the detector. As expected, the drift angle must be

$$\mathrm{tg}\Theta_L=\mu H\cdot 10^{-4},$$

where μ is the carrier mobility, and H (T) is the magnetic field.

At magnetic field strength 1.68 T, a systematic displacement of the measured coordinate by 10 μm (for holes) is observed. In addition, the FWHM of the distribution, determined by the centroid method, increased to 12 μm.

Effect of radiation

There have been quite a number of investigations and publications (see, for example, Refs. 23 and 93–97) devoted to the effects of radiation damage of semiconductor detectors (including track detectors). The structures of the majority of semiconductor track detectors, and also the corresponding electronics include a base material (mainly silicon) and insulating SiO_2 oxide layers. Therefore, the change in the characteristics of the devices as a result of radiation damage is due to the change in the properties of

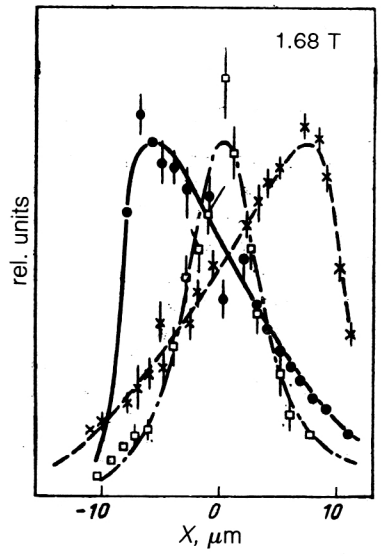

FIG. 26. Charge distribution in a microstrip detector. The open squares show the distribution without a magnetic field, and the crosses and black circles show the distributions in the presence of fields of 1.68 T and −1.68 T, respectively.[54]

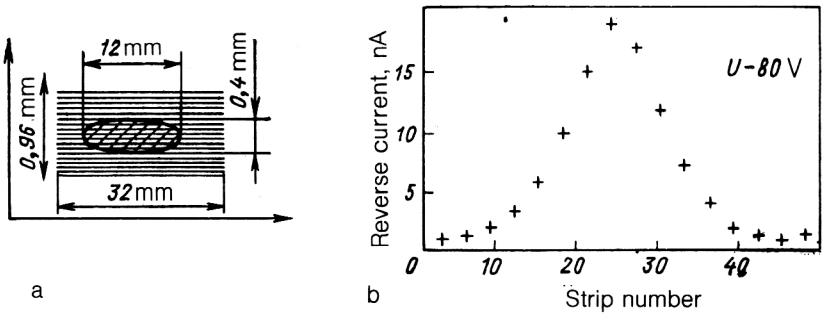

FIG. 27. Influence of radiation damage (2.3×10^{12} particles) on the value of the reverse currents of a microstrip detector: a) position of beam of hadrons (200 GeV) relative to the MSD strips (pitch 20 μm); b) reverse currents of individual strips (they repeat the profile of the beam intensity).[94]

these materials. If an ionizing particle with energy greater than 250 keV passes through the device, damage to the crystal lattice in the base material can occur—atoms can be displaced and knocked out of the lattice sites, and the isotope composition can be changed as a result of nuclear reactions. Such processes lead to the appearance of capture centers and recombination of carriers and to a change of the effective donor or acceptor concentrations in the volume of the semiconductor (at certain doses, the type of conduction may be changed).[93] Because they have a low mobility, the carriers produced in the SiO_2 film as a result of ionization can remain ("undispersed") in the layer, and this changes the electrical properties of the device.

The most characteristic effects that accompany radiation damage of semiconductor detectors are: a) an increase of the reverse current (an increase of the noise) due to the decrease in the lifetime of the minority carriers; b) a decrease in the signal amplitude (the signal-to-noise ratio) because of incomplete collection of the charge; c) a deterioration of the time resolution due to the lowering of the carrier mobility; d) a change in the depletion voltage of the detector due to the change in the effective impurity concentration (resistivity) of the material.

These effects can lead to significant deterioration in the accuracy of the measurement of the particle positions and, at certain doses, may cause failure of the detector. Most investigations show that microstrip detectors can withstand doses (without completely losing their detecting properties) up to several megarads (hundredths of a megagray). Such a dose can be introduced by relativistic particles with $F \simeq 4\times10^{13}$ cm^{-2}.

We shall consider the results of some investigations of the radiation damage of microstrip detectors. In the framework of the NA11/NA32 experiment at CERN, an investigation was made into the characteristics of the microstrip detectors in a telescope consisting of detectors made from n-type silicon with resistivity $\rho=3$ k$\Omega\cdot$cm.[94] The detector thickness was 280 μm, and the strip width was 20 μm. The beam consisted of unseparated hadrons with energy 200 GeV focused onto Be or Si targets. The position of the beam relative to the detectors is shown in Fig. 27a.

During the period 1982–1984, the telescope received irradiation with 2.3×10^{12} particles (the irradiated area was 4.8 mm^2). The dependence in Fig. 27b repeats the distribution of the beam profile—the reverse current of the strips at the center of the beam distribution exceeds by approximately 20 times the dark current at the edge (for comparison, the reverse current before irradiation was 1 nA/strip). The increase in the current satisfies the dependence

$$I_d=I_0+\alpha F,$$

where I_d is measured in nA/cm^2 and F in cm^{-2}; $\alpha=1.3\times10^{-8}$ nA/cm. A similar behavior of the detector currents was observed in other investigations: $\alpha=3\times10^{-8}$ nA/cm in Ref. 95, and $\alpha=9\times10^{-8}$ nA/cm in Ref. 96. The differences between the values of α can be attributed to the difference between the temperature conditions of measurement of the currents, and also possible annealing of defects at room temperature. As was shown in Ref. 96, even at room temperature there is a decrease with time of the currents of a damaged microstrip detector in accordance with the law $I_d = I_0 t^{-0.07}$. Annealing at 80 °C for 24 h gave a decrease of the currents by 12%.

Besides the increase of the reverse current for strips with radiation damage, depletion of the detector at a relatively lower voltage (reduction of the effective donor concentration) was observed.[94] It was also found that there was a decrease of the interstrip resistance in the damaged region due to surface effects, the decrease being from 50 to 2 GΩ. Detectors irradiated in a beam of protons (15 GeV) that had accumulated a dose of several hundredths of a megagray[95] exhibited a decrease of the pulse height of the extracted signal by 10 and 20% for detection of γ rays (59.5 keV from ^{241}Am) and electrons (from ^{90}Sr), respectively.

A local reduction of the effective donor concentration causes the appearance of a transverse component of the electric field in the working volume of the detector. The situation within a completely depleted detector is shown in Fig. 28. The "holes" that arise along the track of the particle (and then follow the field lines) will be displaced within the damaged region. Figure 28 shows the behavior of the mean difference between the measured and predicted coordinate in a damaged detector (for individual events, the uncertainty in the prediction of the particle position was 2 μm, and the random error in the measurement of the coordinate was 5 μm). The measured coordinate was shifted within the central region of the detector, where the radiation damage was greater. In Ref. 94, expressions are given for the description of these processes, and also a method for calculating the corrections for position measurements. The results obtained there indicate that the ad-

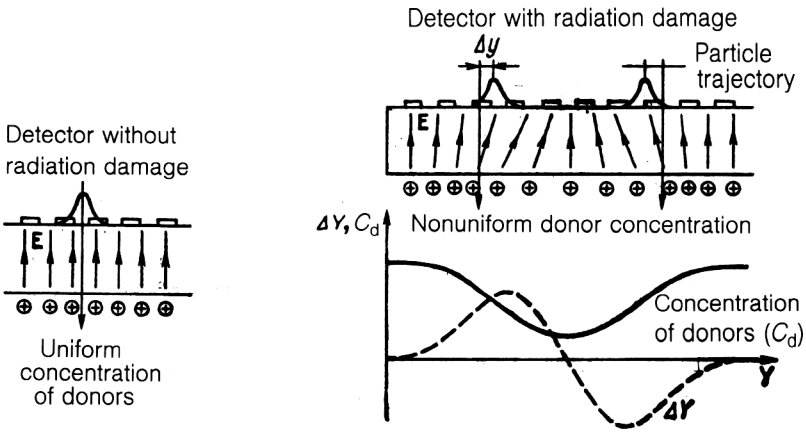

FIG. 28. Influence of local radiation damage nonuniform over the area of an MSD on the accuracy of determination of the particle position.[94]

missible increase of the currents of a microstrip detector can be ignored up to a dose level of 0.01 MGy ($F \sim 4 \times 10^{13}$ cm^{-2}). However, if the depletion is not uniform over the area of the detector, fluxes of order 10^{13} cm^{-2} may give rise to significant inaccuracies in the position measurement.

The radiation damage of position detectors based on CCDs and drift chambers has not been sufficiently investigated, but it is probable that the conclusions obtained for microstrip detectors will largely be true for these detectors too. Note that devices that use standard MIS structures (CCD detectors and electronics in MOS technology) are more sensitive to radiation damage and can withstand doses of not more than 0.1 kGy.[93] However, as was shown in Ref. 97, the radiation dose of the primary electronics can be increased to 0.1 MGy (Si) if special technologies that improve the radiation hardness of the SiO_2 layer are used. In addition, use of the silicon JFET and GaAs–MESFET make it possible to take radiation doses up to 1 MGy.

7. THE USE OF MINIATURIZED SEMICONDUCTOR TRACK DETECTORS IN EXPERIMENTAL PHYSICS

The development of miniaturized semiconductor detectors (microstrip, CCD, drift chambers) led to the creation, in experimental facilities, of complex semiconductor systems (active targets, vertex detectors, beam spectrometers, etc.) that most fully satisfied the requirements for high-resolution internal detectors. In addition, when they are used it is possible to improve the momentum resolution in the central detectors.

We consider some specific fields of study and experimental facilities using the semiconductor track method.

Fixed-target experiments

One of the first successful experiments using semiconductor track detectors was the NA1 experiment (FRAMM collaboration)[98]—the measurement of the D^+D^- lifetime at the SPS accelerator at CERN. Analysis of the experimental method demonstrated the possibility of measuring the lifetime of short-lived charmed particles by means of a telescope of thin silicon detectors. The target was a multilayered silicon detector with 40 planar detectors measuring 20×20 mm, thickness 300 μm of the sensitive region, and segmentation of the sensitive region into four elements in order to lower the total capacitance of the detector (5×20 mm with a gap of 100 μm). The result of the experiment was the identification of approximately 100 events with D^+D^- production.

The semiconductor method was most widely used in experiments to investigate charmed particles (NA11/NA33, CERN, SPS).[99] The investigation of charmed particles, with lifetime of order 10^{-10} sec, requires detectors with very high spatial resolution (a few microns). In the experiment, several semiconductor methods were used: measurement of the spatial characteristics of the incident beam, detection of the change in the multiplicity in the process of interaction, and measurement of the trajectories of the secondary particles from the vertices. The tracks from the measurements were approximated to vertices in order to find coherent events. The semiconductor part of the experimental facility—the "vertex" detector—is shown schematically in Fig. 29.

The monitor of the incident beam consisted of seven planes of microstrip detectors B_1–B_7 (the orientation of the detectors is shown in Fig. 29a) with strip pitch 20 μm, sensitive area measuring 26×26 mm, and thickness 300 μm. The accuracy in the measurement of the position of the incident beam (200 GeV/c) was 5 μm along the vertical and 20 μm along the horizontal. The active target (Fig. 29b) consisted of 14 planes of microstrip detectors with separation 500 μm between them. The microstrip detectors of the active target had strip pitch 20 μm, thickness 280 μm of the sensitive region, and dimensions 26×26 mm. The signals from the active target were used to organize the first-level trigger.

The vertex detector consisted of eight planes of microstrip detectors V_1–V_8 (the orientation is shown in Fig. 29a) and two detectors based on CCDs (Fig. 29c). The microstrip detectors had strip pitch 25 μm and measured 24×36 mm. The detectors based on the two-coordinate CCDs had pixels measuring 22×22 μm, area 1 cm^2 of the sensitive surface, and effective thickness 15 μm. The spatial resolution of the CCD detectors was $\sigma \simeq 5$ μm, and that of the microstrip detectors was $\sigma \simeq 5$–10 μm. The data readout

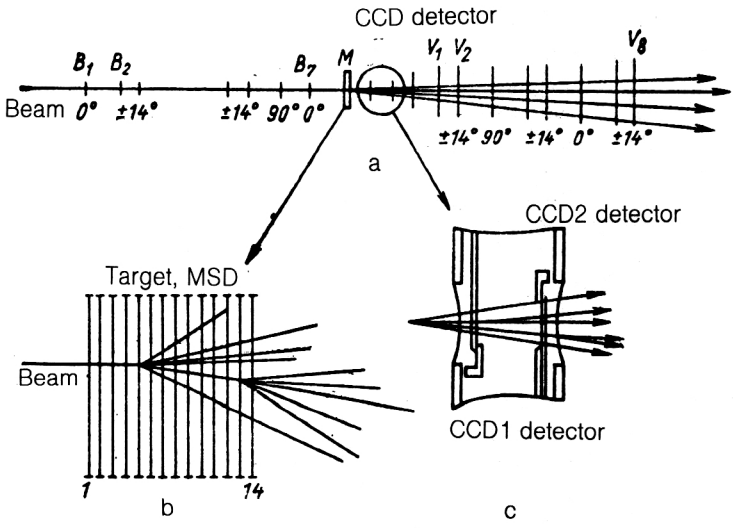

FIG. 29. Schematic form of vertex detector of the facility NA11/NA32 at CERN (Ref. 99): a) vertex part; b) active target; c) vertex CCD detector.

from the microstrip detectors was by means of capacitative charge division. This experimental facility permitted accurate spatial reconstruction of both the primary and secondary interaction vertices and made it possible to reduce considerably the influence of the background substrate.

Structurally similar vertex detectors based on semiconductor track detectors have been used in many experimental facilities with fixed targets. Table VII gives generalized data on the use of the semiconductor track method in a number of modern experiments.

Colliding-beam experiments

In the physics of superhigh energies, in which the investigations are currently developing at colliders, semiconductor track detectors also occupy a prominant place.

The DELPHI vertex detector (CERN, LEP).[100] The detector consists of two coaxial cylindrical surfaces formed of microstrip detectors that surround the interaction region (Fig. 30). Each cylindrical surface contains 24 modules (four microstrip detectors in each module). The parameters of the microstrip detectors are as follows: sensitive region 58×32 and 58×25.6 mm, thickness 300 μm, strip pitch 20 μm, readout pitch 60 μm. The readout from the microstrip detectors is made by means of MICROPLEX circuits and the method of capacitative charge division. The total area of the sensitive surface of the DELPHI vertex detector is 0.332 m^2, the total number of readout outputs is 55 296, and the number of integrated circuits of the MICROPLEX readout is 432. The spatial resolution of the detector is 5 μm.

The MARK II vertex detector (SLAC, SLC).[101] The main requirements that were taken into account in the development of the vertex detector MARK II were the obtaining of a high efficiency for detection of particles with momenta 1–2 GeV/c, a spatial resolution not worse than 20 μm, a double-particle resolution not worse than 150 μm, and minimal size of the region occupied by the detector (the parameters of the vertex region of interaction at SLC are as follows: radius of vacuum chamber 26 mm, length 280 mm, and external diameter of detector limited by the internal dimension 44 mm of the vertex drift chamber).

TABLE VII. Examples of experiments using miniaturized semiconductor track detectors.

Experiment	Target	Track detector	Semiconductor detector trigger
NA1, CERN	40 MSDs: active target		
NA11/32, CERN	10–14 MSDs: active target	7 MSDs–beam monitor (2 CCD detectors+ 8 MSDs)–vertex detector	Microprocessor of active target
NA19, CERN	Emulsion	6 MSDs–beam monitor 7 MSDs–vertex detector	
WA71, CERN	Emulsion +2 telescopes of five semiconductor detectors	2 MSDs–beam monitor 6 MSDs–vertex detector	From change in multiplicity (2 semiconductor-detector telescopes)
P696, Fermilab	40 MSD active target +2 semicondcutor detector telescopes	2 MSDs–beam monitor 8 MSDs–vertex detector	The same
E653, Fermilab	Emulsion	2 MSDs–beam monitor 21 MSDs–vertex detector 9 MSDs–small-angle detector	

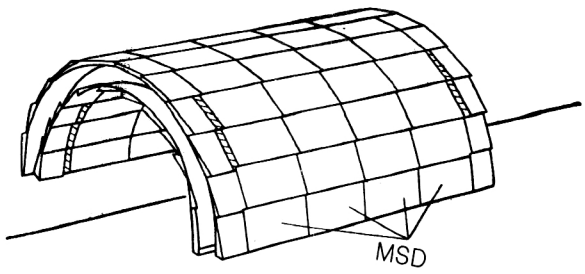

FIG. 30. Fragment of the vertex detector of the DELPHI facility, CERN (96 MSDs, strip pitch 20 μm, readout pitch 60 μm, total area of sensitive surface 0.332 m^2).[100]

The schematic form of the vertex detector MARK II is shown in Fig. 31. It consists of three cylindrical layers of microstrip detectors (36 detector modules). The radii of the cylinders are 28, 33, and 37 mm. The strip pitches are 25, 29, and 33 μm. The strips are orientated parallel to the beam axis. The information readout is by means of MICROPLEX circuits placed constructively at the ends of the cylindrical planes. The total number of readout outputs is 18 000.

There is a project for a MARK II vertex detector using CCD detectors.[102] The detector is a spatial structure of 24 planes, each of which consists of five coordinate detectors based on a CCD.

Vertex detector in the ALEPH experiment (CERN, LEP).[42,103] This has two cylindrical layers of radius 90 and 120 mm, which are set up directly in the vacuum chamber of the collider in the region of interaction of the colliding beams. A feature of the ALEPH vertex detector is the use of two-coordinate semiconductor microstrip detectors. The total number of microstrip detectors is 112. The readout is by means of detector electronics in integrated technology (CAMEX 64). The total number of readout outputs is 81 000, and the number of employed CAMEX 64 integrated circuits is 1344. The spatial resolution of the vertex detector is 6 μm.

The record hitherto is the project of a semiconductor vertex detector for experiments planned in the United States with the SSC supercollider.[104] The detector is based on eight paired cylindrical surfaces (Fig. 32) of two-coordinate microstrip detectors (pitch 25 μm of the MSDs)

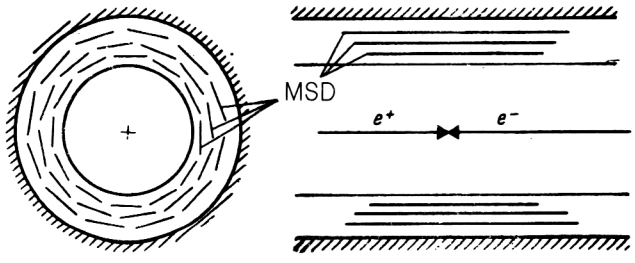

FIG. 31. Arrangement of vertex detector of the facility MARK II, SLAC (36 MSDs measuring 14×74–18×94 mm and pitch 25–33 μm).[101]

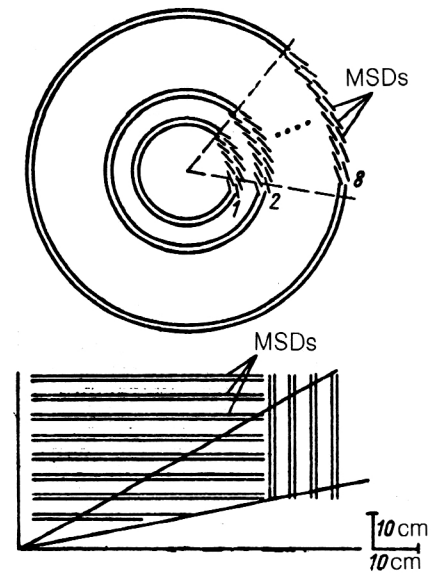

FIG. 32. Arrangement of one of proposed projects for vertex detector for experiments at the planned SSC collider in the United States (the active area of the eight paired cylinders of two-coordinate MSDs is 30 m^2).[104]

with total area 30 m^2. The expected spatial resolution is 6 μm, the double-particle resolution is 100 μm, and the admissible load is 10^8 events/sec.

CONCLUSIONS

The analysis made in this review of results in the development of semiconductor position-sensitive radiation detectors and of the ideas that have been developed for using semiconductor track detectors in experimental physics enables us to draw some general conclusions and predict the future development of such devices.

1. In the eighties, there was a qualitative jump in the traditional use and in the method of creating semiconductor track detectors. The rapid introduction of such detectors into high-energy physics experiments, needing record spatial resolution (and a high counting rate and the possibility of an electronic trigger), gave rise to a considerable number of investigations and the development of new types of STDs, in particular miniaturized STDs (microstrip detectors, semiconductor drift chambers, CCD detectors with deep depletion, etc.), which made it possible to achieve a spatial resolution of detection down to a few microns.

2. The greatest popularity has been achieved by the microstrip detectors, above all because they have an active area (10–30 cm^2) larger than other types of STDs. At the same time, the obvious advantages of CCD detectors [two-dimensional image of the position of the particle track with $\sigma \leqslant 5$ μm, better double-particle resolution, and minimal number of readout outputs (1–50) with the number of elements of order 10^5] may be a decisive factor in their choice, particularly in cases when the integrated doses do not exceed 0.1–10 kGy.

3. As yet, semiconductor drift chambers (in their originally proposed form) have not been used in actual experiments. However, the actual idea of such detectors has been very fruitful and has brought to life many original developments, in particular, matrix devices that combine in a single cell a detector and transistor (see, for example, Ref. 64). In our view, there is no doubt about the prospects for the development of such detectors.

4. The development of miniaturized STDs and the investigations made with them have strongly influenced the technology of the production of semiconductor detectors as a whole as well as the development of multichannel low-noise systems of data readout. The popularity of discrete STDs in the physics of intermediate and low energies is increasing.

5. The projects of future experiments in high-energy physics in which the use of STDs is planned, in particular at the SSC collider in the United States, come up against two limiting factors of no small importance: the total dissipated power of the primary electronics (the planned number of readout channels greater than 10^5 leads to a dissipated power of not less than 50 kW) and the radiation dose of the STDs themselves as well as the primary electronics (the expected dose, Gy/yr from secondary particles in the collider is $3\times 10^5/r^2$ at luminosity 10^{33} cm$^{-2}\cdot$sec^{-1}, where r is the distance from the beam in centimeters).[95]

6. In contrast to the West, where there is significant progress in the development and use of miniaturized STDs, investigations with such detectors in our country is at the initial stage. There are few reports of developments of microstrip detectors (see, for example, Refs. 45–47). There is still the problem of adequate readout electronics.

We should like to thank M. G. Gornov, L. S. Barabash, and Yu. B. Gurov for helpful discussions and comments, S. V. Besfamil'nyĭ for assistance and for verifying some results and statements made in the paper, and V. A. Stankevich for making it possible to investigate individual questions of technology and spectrometry on actual samples of microstrip detectors.

[1] E. Lassgaard, Nucl. Instrum. Methods **162**, 93 (1979).
[2] V. G. Sandukovskiĭ, Preprint 13-82-90 [in Russian], JINR, Dubna (1982).
[3] Yu. K. Akimov, O. V. Ignat'ev, A. I. Kalinin, and V. I. Kushniruk, *Semiconductor Detectors in Experimental Physics* [in Russian] (Énergoatomizdat, Moscow, 1989).
[4] P. G. Rancoita, J. Phys. G **10**, 299 (1984).
[5] V. Radeka, Nucl. Instrum. Methods **226**, 209 (1984).
[6] C. Damerell, Nucl. Instrum. Methods **226**, 26 (1984).
[7] R. Klanner, Nucl. Instrum. Methods **235**, 209 (1985).
[8] P. G. Rancoita and A. Seidman, Riv. Nuovo Cimento **5**, No. 7 (1982).
[9] A. Menzione, Preprint PI/AE 86.8, INFN, Pisa (1986).
[10] A. H. Walenta, Nucl. Instrum. Methods **253**, 558 (1987).
[11] A. G. Chilingarov, Preprint 90-113 [in Russian], Institute of Nuclear Physics, Siberian Branch, USSR Academy of Sciences, Novosibirsk (1990).
[12] P. G. Rancoita and A. Seidman, Preprint CERN-EP/86-113, Geneva (1990).
[13] P. Rehak, Nucl. Instrum. Methods **211**, 323 (1983).
[14] D. Coon, E. Engels, J. D. Plants *et al.*, Nucl. Instrum. Methods **226**, 169 (1984).
[15] W. Vernon, *Proc. of the Workshop: Silicon Detectors for High Energy Physics* (Fermilab, 1981), p. 185.
[16] E. H. M. Heijne and P. Jarron, Nucl. Instrum. Methods **A275**, 467 (1989); F. Krummenacher, C. C. Enz, M. Declercq *et al.*, Nucl. Instrum. Methods **A288**, 176 (1990).
[17] E. E. Haller, IEEE Trans. Nucl. Sci. **NS-29**, 1109 (1982); J. T. Walton, Nucl. Instrum. Methods **226**, 1 (1984).
[18] K. H. Lauterjung, J. Pokar, B. Schimmer *et al.*, Nucl. Instrum. Methods **22**, 117 (1963); R. Bock, Nucl. Instrum. Methods **41**, 190 (1966).
[19] E. Mathieson, Nucl. Instrum. Methods **97**, 171 (1971).
[20] R. B. Owen and M. L. Awcock, IEEE Trans. Nucl. Sci. **NS-15**, 290 (1968); S. Kabitzer and W. Melzer, IEEE Trans. Nucl. Sci. **56**, 301 (1967).
[21] A. Doehring, S. Kalbitzer, W. Melzer *et al.*, IEEE Trans. Nucl. Sci. **59**, 40 (1968); J. R. Gigante, IEEE Trans. Nucl. Sci. **111**, 345 (1973); J. L. Alberi and V. Radeka, IEEE Trans. Nucl. Sci. **NS-23**, 251 (1976).
[22] J. Kemmer, Nucl. Instrum. Methods **169**, 499 (1980); **226**, 89 (1984).
[23] C. Barbiellini, P. Buksh, G. Cecchet *et al.*, Nucl. Instrum. Methods **235**, 216 (1985).
[24] W. W. Daenick, Phys. Rev. **177**, 1763 (1969).
[25] J. U. Anderson, K. O. Nielsen, J. Skak-Nielsen *et al.*, Nucl. Phys. **A241**, 317 (1975); J. U. Andersen, Phys. Rev. Lett. **36**, 1539 (1976).
[26] W. Augustyniak, C. Borcea, M. Lewitowicz *et al.*, Z. Phys. A **332**, 209 (1989).
[27] W. H. Berlinger, IEEE Trans. Nucl. Sci. **NS-21**, 374 (1974).
[28] J. Adam, D. Venos, A. Kuklik *et al.*, Nucl. Instrum. Methods **228**, 79 (1985).
[29] A. Feuerstein and S. Kalbitzer, Nucl. Instrum. Methods **109**, 601 (1973); R. V. Strikantiah, J. Phys. E **15**, 171 (1982).
[30] E. Bel'tsazh, B. P. Osipenko, and V. G. Sandukovskiĭ, Preprint 13-82-91 [in Russian], JINR, Dubna (1982); B. Amov, A. Dzhakov, V. P. Osipenko *et al.*, Prib. Tekh. Eksp. No. 3, 57 (1985).
[31] L. S. Barabash, E. Belcarz, Y. B. Gurov *et al.*, Nucl. Instrum. Methods **A288**, 375 (1990).
[32] W. K. Hofker, D. P. Oosthoek, A. M. E. Hoeberechts *et al.*, IEEE Trans. Nucl. Sci. **NS-13**, 208 (1966).
[33] J. S. Fleming, Nucl. Instrum. Methods **150**, 417 (1978); G. Riepe and D. Protic, Nucl. Instrum. Methods **226**, 103 (1984).
[34] J. A. den Boer, A. M. E. Hoeberechts, W. K. Hofker *et al.*, Nucl. Instrum. Methods **92**, 173; T. Davinson, A. C. Shotter, E. W. Macdonald *et al.*, Nucl. Instrum. Methods **A288**, 245 (1990).
[35] E. Gatti and P. F. Manfredi, Riv. Nuovo Cimento **9**, 25 (1986).
[36] E. H. M. Heijne, L. Hubbeling, B. D. Hyams *et al.*, Nucl. Instrum. Methods **178**, 331 (1980).
[37] M. Caccia, L. Evensen, T. E. Hansen *et al.*, Preprint CERN-EP/87-81, Geneva (1987).
[38] S. R. Amendolia, F. Bedeschi, E. Bertolucci *et al.*, Nucl. Instrum. Methods **226**, 117 (1984).
[39] D. Gutknecht, Nucl. Instrum. Methods **288**, 13 (1990).
[40] B. Deal, IEEE Trans. ED. **Ed-27**, 606 (1980).
[41] G. Bagliesi, G. Batignani, L. Bosisio *et al.*, Preprint PI/AE 87/2, INFN, Pisa (1986); L. Bosisio, E. Focardi, F. Forti *et al.*, Preprint PI/AE 87/2, INFN, Pisa (1987).
[42] P. Holl *et al.*, IEEE Trans. Nucl. Sci. **NS-36**, 251 (1988).
[43] R. Henck, Nucl. Instrum. Methods **A288**, 278 (1990).
[44] Micron Semiconductor LTD (1989).
[45] I. P. Barkov, I. M. Gazizov, L. L. Kurchaninov *et al.*, Preprint 90-65 [in Russian], Institute of High Energy Physics, Protvino (1990).
[46] V. I. Astakhov, A. Bishoff, A. S. Vodop'yanov *et al.*, Preprint R13-90-7 [in Russian], JINR, Dubna (1990).
[47] B. D. Dvornikov, A. A. Kochenova, V. B. Kuryatkov *et al.*, Preprint 1646 [in Russian], Leningrad Institute of Nuclear Physics, Leningrad (1990).
[48] J. B. A. England, B. P. Hyams, L. Hubbeling *et al.*, Nucl. Instrum. Methods **185**, 43 (1981).
[49] V. Radeka and R. Boie, Nucl. Instrum. Methods **178**, 543 (1980).
[50] G. Apollinari, F. Bedeschi, G. Bellettini *et al.*, Nucl. Instrum. Methods **A253**, 537 (1987).
[51] S. R. Amendolia, F. Bedeshi, and E. Bertolucci, Nucl. Instrum. Methods **226**, 82 (1984).
[52] E. H. M. Heijne, Preprint 83-06, CERN, Geneva (1983).
[53] C. Adolphsen, A. Litke, A. Schwarz *et al.*, Nucl. Instrum. Methods **A253**, 444 (1987).
[54] E. Belau, R. Klanner, G. Lutz *et al.*, Nucl. Instrum. Methods **214**, 253 (1983).

[55] B. Hyams, U. Kotz, E. Belau *et al.*, Nucl. Instrum. Methods **205**, 99 (1983).
[56] W. R. Th. Ten Kate, Nucl. Instrum. Methods **A253**, 333 (1987).
[57] M. Anghinolfi, M. Castoldi, and A. Rottura, Nuovo Cimento **98A**, 551 (1987).
[58] E. F. Gatti and P. Rehak, Nucl. Instrum. Methods **225**, 608 (1984).
[59] P. Rehak, E. Gatti, A. Longoni *et al.*, Nucl. Instrum. Methods **A235**, 223 (1985).
[60] E. Gatti, P. Rehak, and J. T. Walton, Nucl. Instrum. Methods **226**, 129 (1984).
[61] P. Rehak, J. Walton, and E. Gatti, Nucl. Instrum. Methods **A248**, 367 (1986).
[62] P. N. Luke, N. W. Madden, F. S. Goulding *et al.*, IEEE Trans. Nucl. Sci. **NS-32**, 457 (1985).
[63] E. Gatti, P. Rehak, and J. Kemmer, Nucl. Instrum. Methods **A253**, 511 (1987).
[64] J. Kemmer and G. Lutz, Nucl. Instrum. Methods **A253**, 365 (1987); J. Kemmer, G. Lutz, U. Prechtel *et al.*, Nucl. Instrum. Methods **A288**, 92 (1990).
[65] K. J. Rawlings, Nucl. Instrum. Methods **A253**, 85 (1986); **A256**, 297 (1987); **A260**, 346 (1987).
[66] L. Struder, P. Holl, G. Lutz, and J. Kemmer, Preprint MPI-PAE/Exp. E1 166, Munich (1986).
[67] J. Kemmer, Nucl. Instrum. Methods **A288**, 282 (1990).
[68] W. S. Boyle and G. E. Smith, Bell Syst. Tech. J. **49**, 587 (1970); G. F. Amelio, M. F. Tompsett, and G. E. Smith, Bell Syst. Tech. J. **49**, 593 (1970).
[69] C. J. S. Damerell, F. J. M. Farley, A. R. Gillman, and F. J. Wickens, Nucl. Instrum. Methods **185**, 33 (1981).
[70] R. Bailey, C. J. S. Damerell, R. L. English *et al.*, Nucl. Instrum. Methods **213**, 201 (1983).
[71] M. H. White, D. R. Lampe, F. C. Blaha, and I. A. Mack, IEEE J. Solid-State Circuits **SC-9**, 1 (1974).
[72] C. J. S. Damerell, R. L. English, A. R. Gillman *et al.*, Nucl. Instrum. Methods **A288**, 236 (1990).
[73] A. Benetello, G. Calvelli, G. Zanella *et al.*, Nucl. Instrum. Methods **258**, 235 (1987).
[74] L. Struder, H. Brauninger, M. Meier *et al.*, Nucl. Instrum. Methods **A288**, 227 (1990).
[75] G. Bellini, P. Angelo, P. Iuzani *et al.*, Nucl. Instrum. Methods **196**, 351 (1982); A. Menzione, Preprint PI/AE 86/8, INFN, Pisa (1986).
[76] S. Benso, M. Dameri, G. Diambrini-Palazzi *et al.*, Nucl. Instrum. Methods **291**, 351 (1982).
[77] E. H. M. Heijne and P. Jarron, Nucl. Instrum. Methods **226**, 12 (1984); W. Buttler, G. Lutz, V. Liberali *et al.*, Nucl. Instrum. Methods **A288**, 140 (1990).
[78] K. Ogava, Bell Syst. Tech. J. No. 62, 1181 (1983).
[79] J. Honthoff and T. H. Uittenbogard, Electr. Components Appl. No. 1, 42 (1982).
[80] A. Alessangrello, C. Brafferio, P. V. Camin *et al.*, Nucl. Instrum. Methods **A289**, 426 (1990).
[81] E. Gatti and P. F. Manfredi, Nucl. Instrum. Methods **A226**, 142 (1984).
[82] B. J. Hosticka, Nucl. Instrum. Methods **A226**, 185 (1984).
[83] J. T. Walker, S. Parker, R. Hyams *et al.*, Nucl. Instrum. Methods **A266**, 200 (1984).
[84] W. Buttler, B. J. Hosticka, G. Lutz *et al.*, Nucl. Instrum. Methods **A288**, 187 (1990).
[85] J. C. Stanton, IEEE Trans. Nucl. Sci. **NS-36**, 522 (1989).
[86] W. C. Carithers, R. P. Ely, C. Haber *et al.*, Nucl. Instrum. Methods **A289**, 388 (1990).
[87] G. Lutz, W. Buttler, H. Bergmann *et al.*, Nucl. Instrum. Methods **A263**, 163 (1988).
[88] W. Buttler, G. Lutz, and H. Bergmann, Preprint MPI-PAE/Exp. E1. 178, Munich (1987).
[89] E. Benville, K. Borer, E. Chesi *et al.*, Nucl. Instrum. Methods **A288**, 157 (1990).
[90] P. Rehak, S. Rescia, V. Radeka *et al.*, Nucl. Instrum. Methods **A288**, 168 (1990).
[91] R. J. Yarema and T. Zimmerman, IEEE Trans. Nucl. Sci. **NS-37**, 430 (1990).
[92] G. Gollin, M. V. Isailo, F. C. Shoemaker *et al.*, IEEE Trans. Nucl. Sci. **NS-26**, 59 (1979).
[93] V. A. J. Van Lint, Nucl. Instrum. Methods **A253**, 453 (1987).
[94] H. Dietl, T. Gooch, D. Kelsey *et al.*, Nucl. Instrum. Methods **A253**, 460 (1987).
[95] T. Ohsugi, A. Taketani, M. Noda *et al.*, Nucl. Instrum. Methods **A265**, 105 (1989).
[96] P. Borgeaud, J. G. McEwen, P. G. Rancoita, and A. Seidman, Nucl. Instrum. Methods **211**, 363 (1983).
[97] W. R. Dawes, Jr., Nucl. Instrum. Methods **A288**, 54 (1990).
[98] E. Albini, Preprint CERN-EP/82-12, Geneva (1982).
[99] P. Weilhammer, Preprint CERN-EP/86-54, Geneva (1986).
[100] H. Dijkstra, R. Horisberger, L. Hubbeling *et al.*, Nucl. Instrum. Methods **A289**, 400 (1990).
[101] A. Litke, C. Adolphsen, A. S. Schwarz *et al.*, Nucl. Instrum. Methods **A265**, 93 (1988); C. Adolphsen, G. Gratta, L. Labarga *et al.*, Nucl. Instrum. Methods **A288**, 257 (1990).
[102] C. W. Akerlef, J. W. Charpman, I. Gialas *et al.*, Nucl. Instrum. Methods **A260**, 80 (1987).
[103] P. Holl, H. Dietl, J. Fent *et al.*, Nucl. Instrum. Methods **A257**, 587 (1987).
[104] E. Hartmut and W. Sadrozinski, CERN Report CERN 89-10, ECFA 89-124 (1989), p. 297.

Translated by Julian B. Barbour